SUPPORTING INFORMATION

Conformation-Specific Infrared and Ultraviolet Spectroscopy of Cold [YAPAA+H]+ and [YGPAA+H]+ Ions: A Stereochemical "Twist" on the β-Hairpin Turn

Andrew F. DeBlase, Christopher P. Harrilal, John T. Lawler, Nicole L. Burke, Scott A. McLuckey, and Timothy S. Zwier
Department of Chemistry, Purdue University, West Lafayette, Indiana 47907-2084, United States

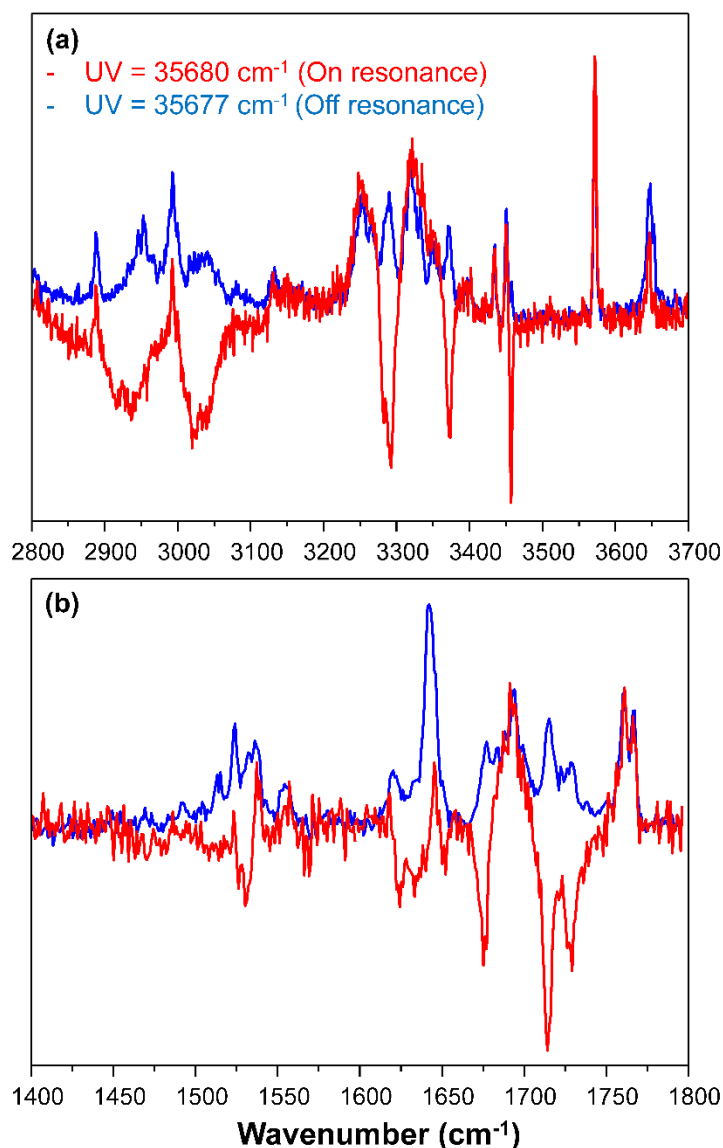## I. Background Subtraction from Conformation-Specific IR Spectra

Figure S.1. A comparison of the raw conformation-specific IR spectra (red traces) taken with the UV laser on resonance with conformer B (35,680 cm⁻¹) to the background non-specific ion gain spectra (blue traces) taken a few wavenumbers off resonance (35,677 cm⁻¹) in the X-H stretching (a) and amide I and II (b) regions of the infrared. The spectra were normalized to the intensities of the stretching transitions of the acid OH and CO groups and were subtracted to give the spectra of conformer B that are reported in the manuscript.
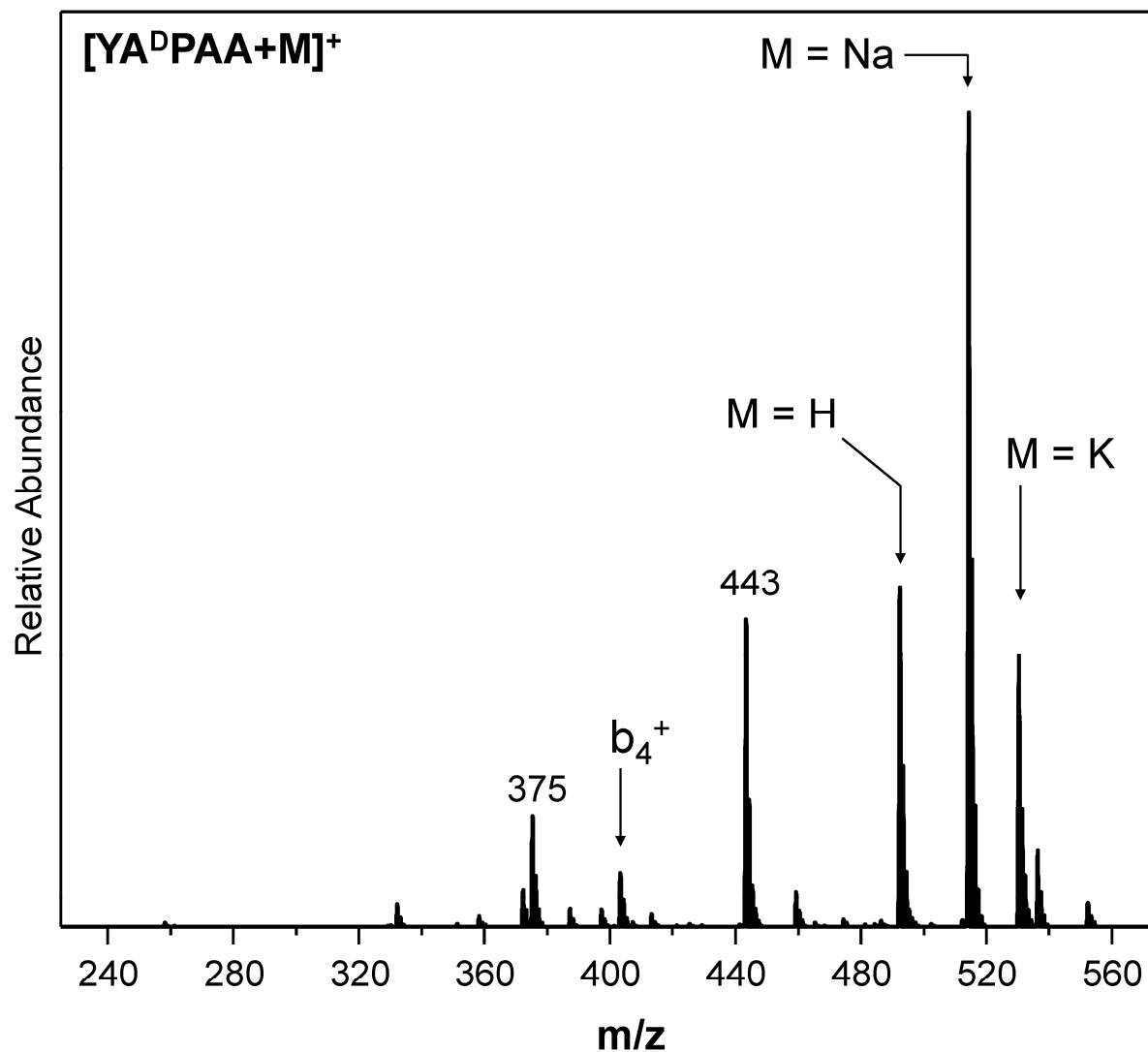
II. Mass Spectra

Figure S.2. Full nESI mass spectrum of YA^{D}PAA electrosprayed from a solution of 50:50 MeOH:H$_2$O. The dominant [YA^{D}PAA+M]$^+$ species are labeled, where M = H, Na, and K. The predominant b$_4^+$ fragment ion is also labeled. The two unidentified peaks (at m/z = 375 and 443) were separated from the precursor [YA^{D}PAA+H]$^+$ ions by an auxiliary broadband notched-chirp pulse isolation in q2 and were not observed upon CID or UVPD of [YA^{D}PAA+H]$^+$.
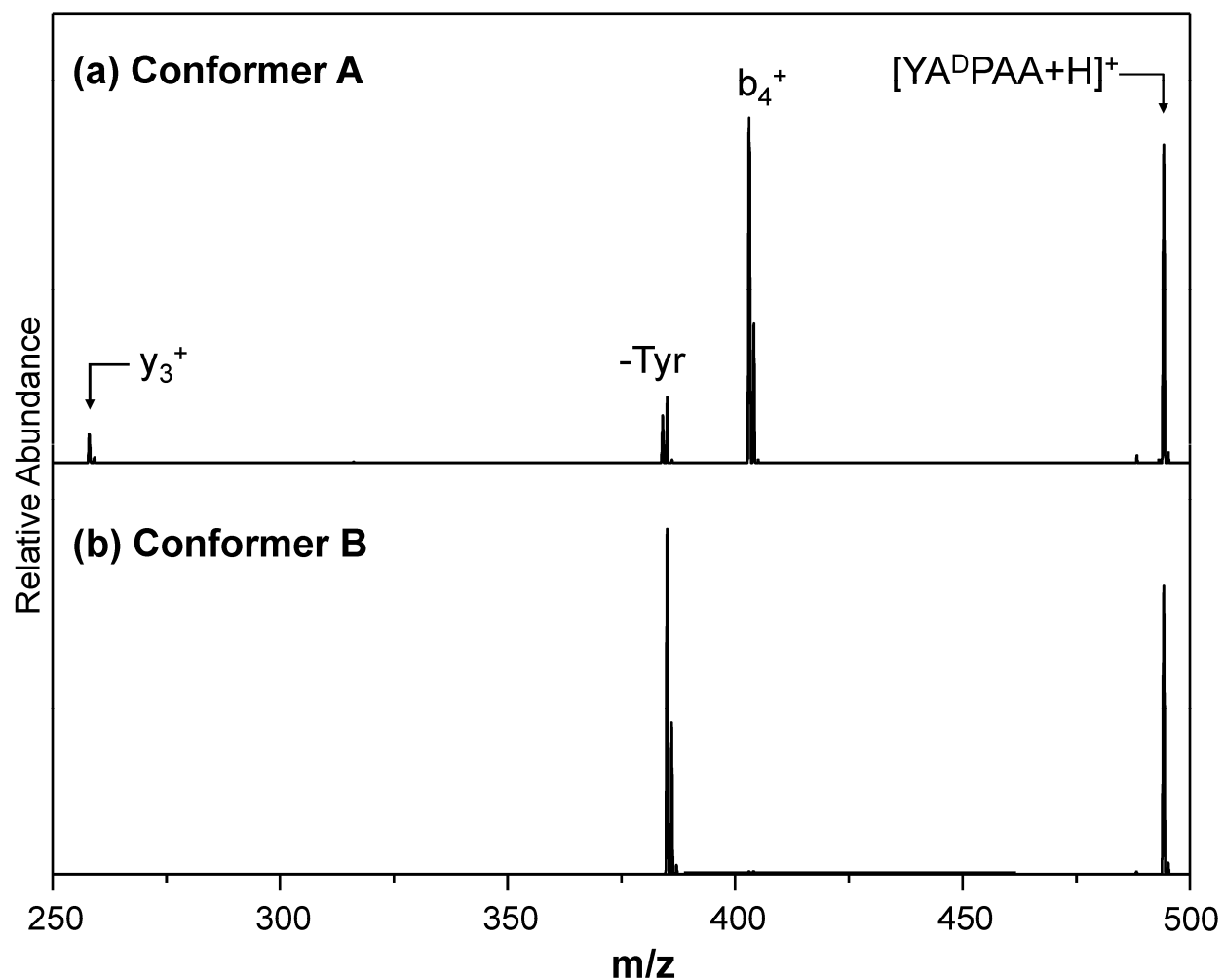
Figure S.3. UVPD mass spectrum of [YADPAA+H]$^+$ taken with the UV laser on resonance with conformers A (a) and B (b). The spectra were acquired by MSAE[1] in high resolution mode (120 ms analysis ramp). Conformer A exhibits much more b$_4^+$ than y$_3^+$, similar to the result observed by Poutsma and coworkers.[2] However, the -107 Tyr sidechain loss dominates in the UVPD mass spectrum of conformer B.
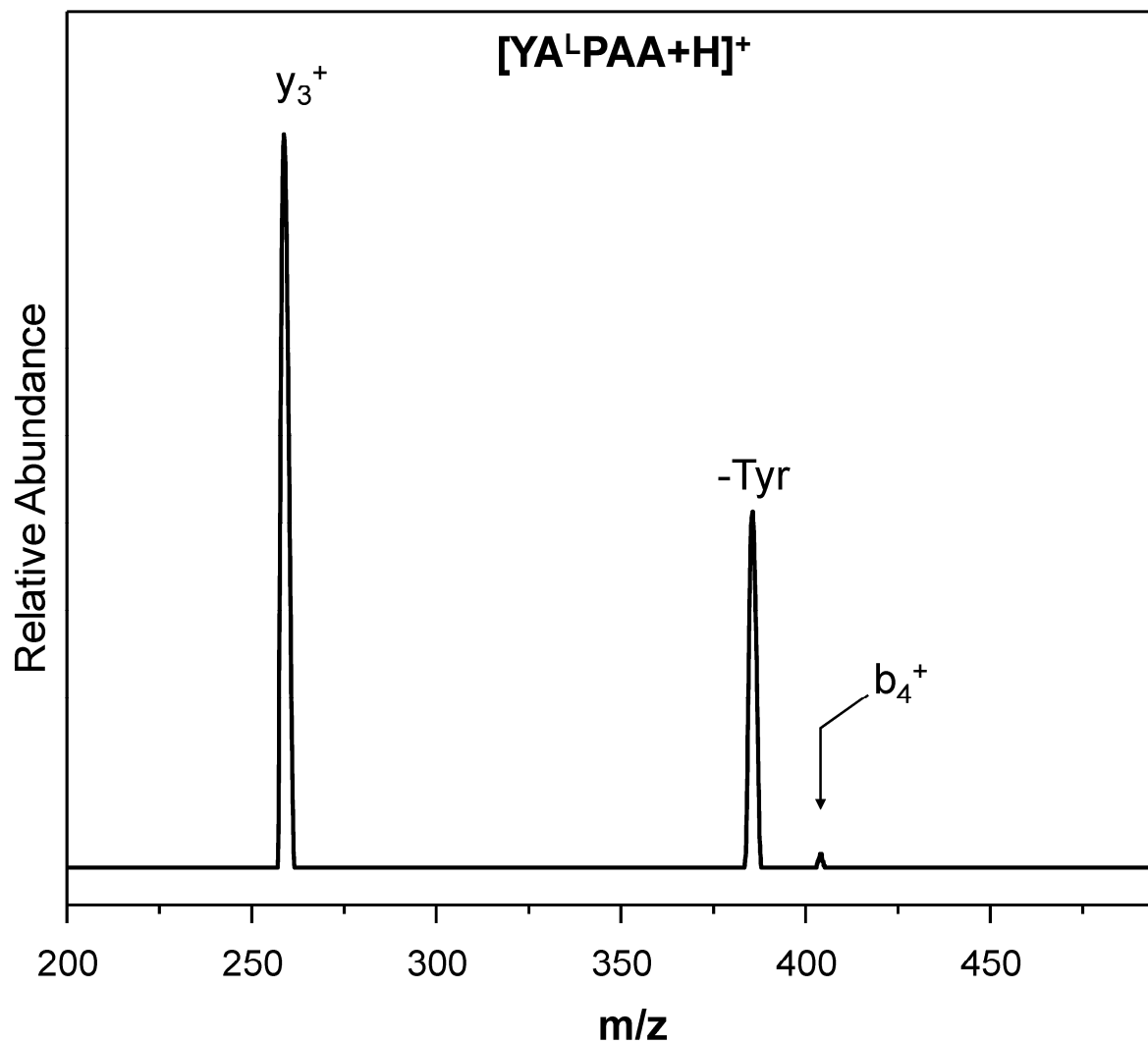
Figure S.4. UVPD mass spectrum of $[YA^LPAA+H]^+$ taken by MSAE[1] in low resolution mode (60 ms analysis ramp). Similar to the observation of Poutsma and coworkers,[2] predominantly y_3^+ over b_4^+ is formed for the L-Pro diastereomer. An abundant -107 fragment resulting from excited state loss of the Tyr sidechain[3] is also observed.

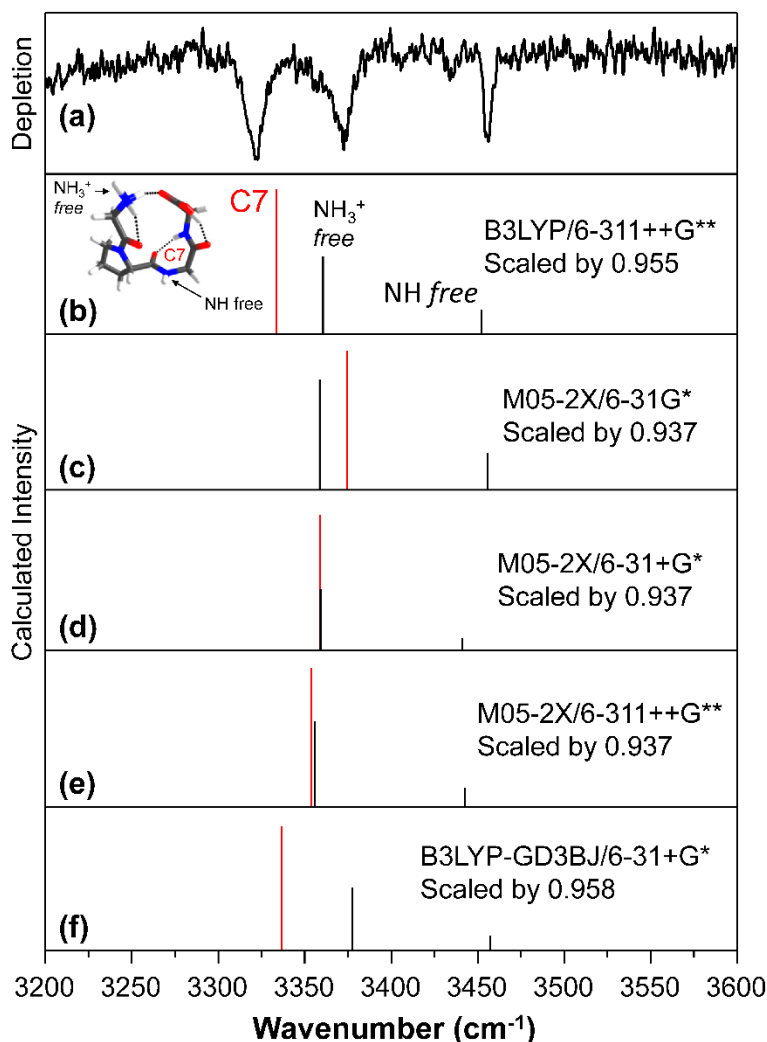## III. Comparison of DFT Harmonic-Level Calculations for [GPGG+H]$^+$

Figure S.5. A comparison of the previously published[4] infrared predissociation spectrum of D$_2$-tagged *trans*-[GPGG+H]$^+$ [structure in (b)], which was isolated from *cis*-[GPGG+H]$^+$ via ion mobility spectrometry,(a) to the calculated harmonic level spectrum at the B3LYP/6-311++G** (b), M05-2X/6-31G* (c), M05-2X/6-31+G* (d), M05-2X/6-31++G** (e), and B3LYP-GD3BJ/6-31+G* levels of theory. The scaling factor for the M05-2X functional (0.937) was consistent with our previous work on [YGGFL+H]$^+$,[5] while the scaling factor for the B3LYP functional (0.955) was consistent with the previous work on [GPGG+H]$^+$ by the Rizzo lab.[4] As both factors brought the free neutral NH stretch into reasonable agreement with the experiment, the scaling factor of 0.958 was derived for the B3LYP-GD3BJ/6-31+G* level of theory using the free NH stretching transition in *trans*-[GPGG+H]$^+$. Note that the wavenumber of the C7 H-bonded NH stretching transition (red) is quite sensitive to the size of the basis set when the M05-2X functional is used, predicting a reversal in the ordering of the C7 and NH$_3^+$ *free* NH stretching transitions when a small basis set is used. The B3LYP functional with the empirical dispersion correction (f) is a less computationally intensive alternative to the large basis set size that yields satisfactory agreement between experiment and theory.
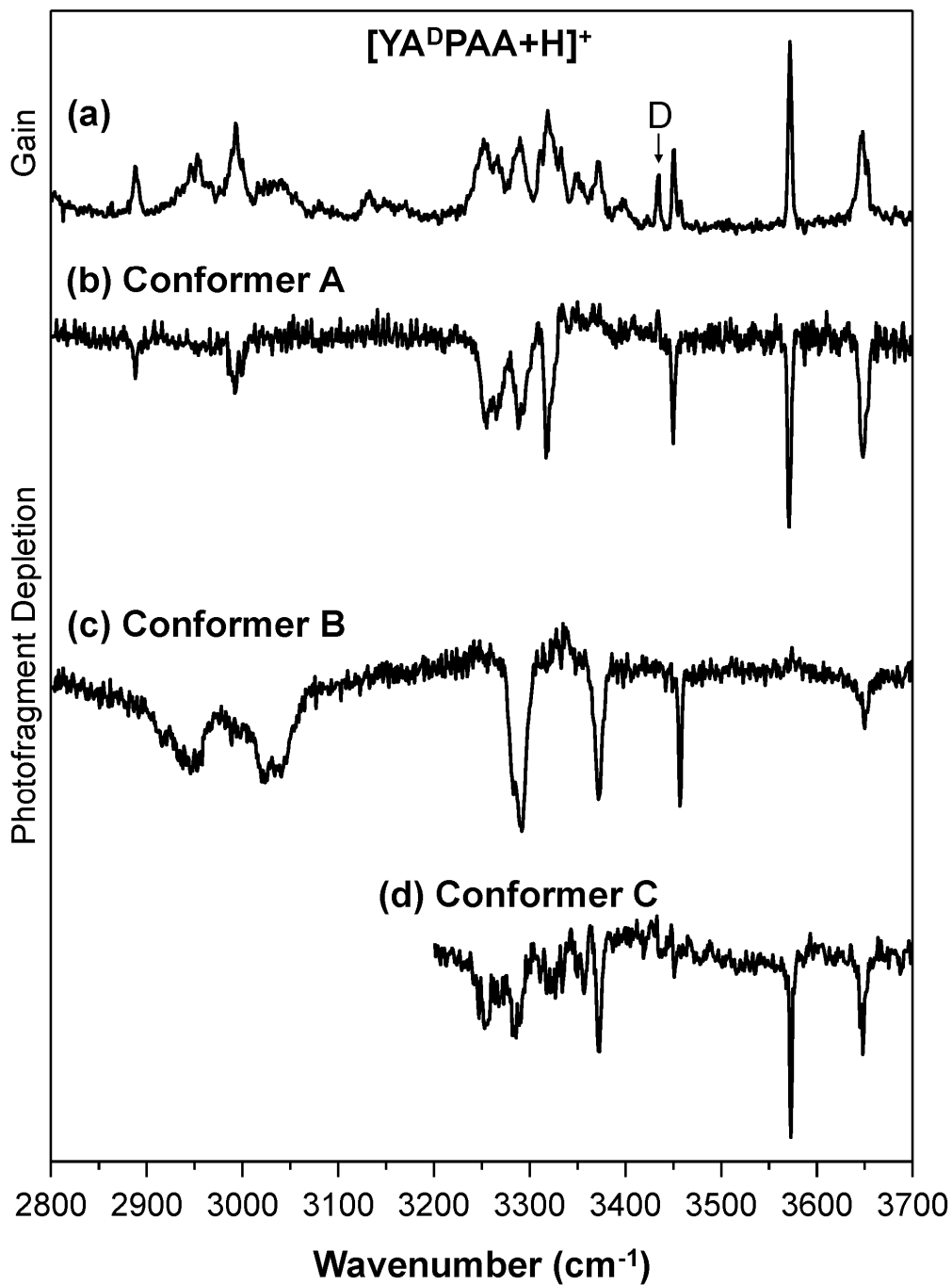
IV. Conformation-Specific IR and UV Spectra of All Conformers

Figure S.6. A comparison of the non-specific infrared photofragment gain spectrum of $[YA^DPAA+H]^+$ (a) to the conformation specific spectra of conformers A (b), B (c), and C (d). With the exception of the band marked D, all transitions are accounted for when combining the infrared spectra of the three conformers.

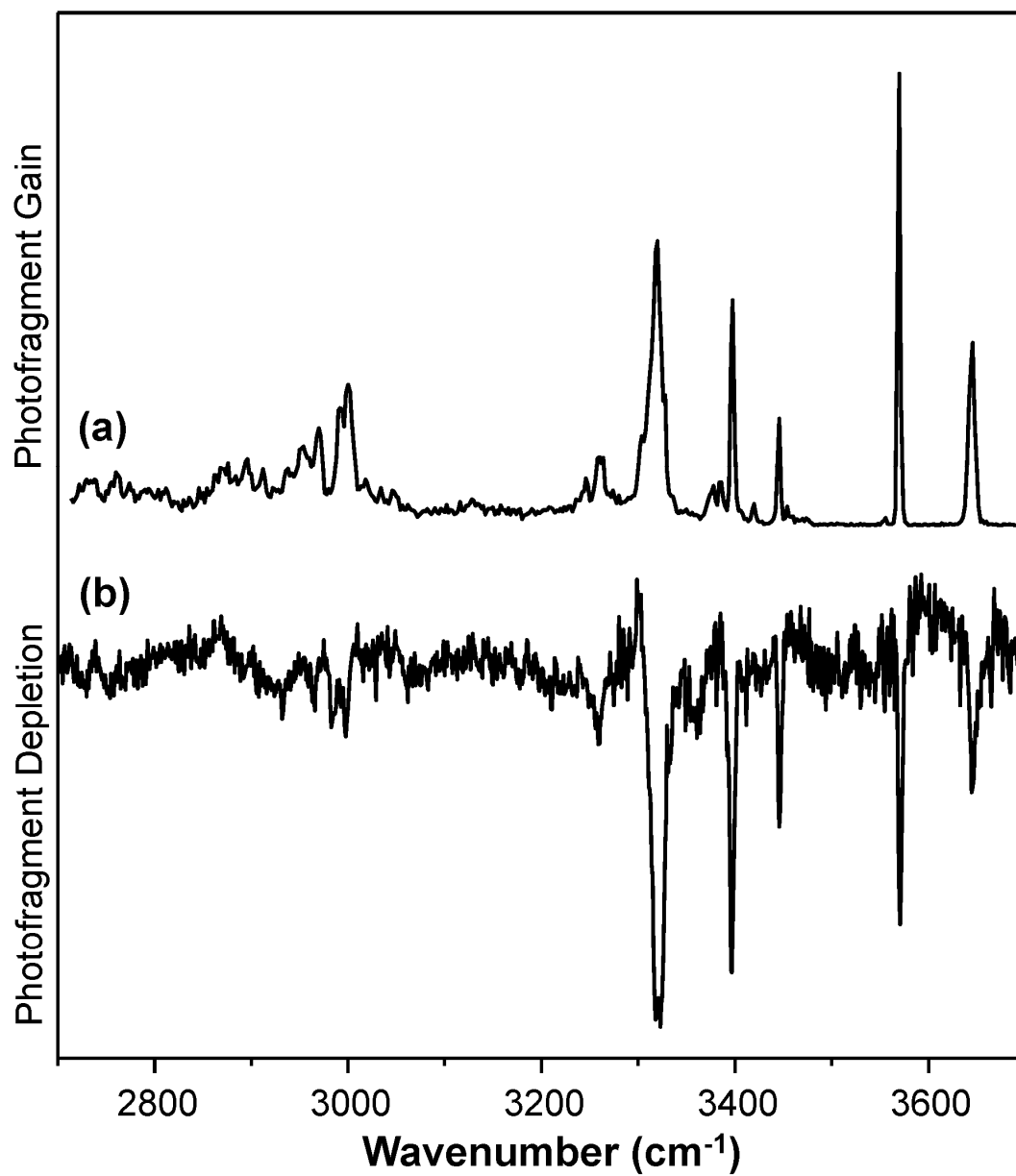**Figure S.7.** A comparison of the infrared photofragment gain spectrum of $[YA^LPAA+H]^+$ to the photofragment depletion spectrum taken on resonance with the most intense transition (35,588 cm^{-1}). Both spectra appear similar, consistent with the presence of one dominant conformer in $[YA^LPAA+H]^+$.
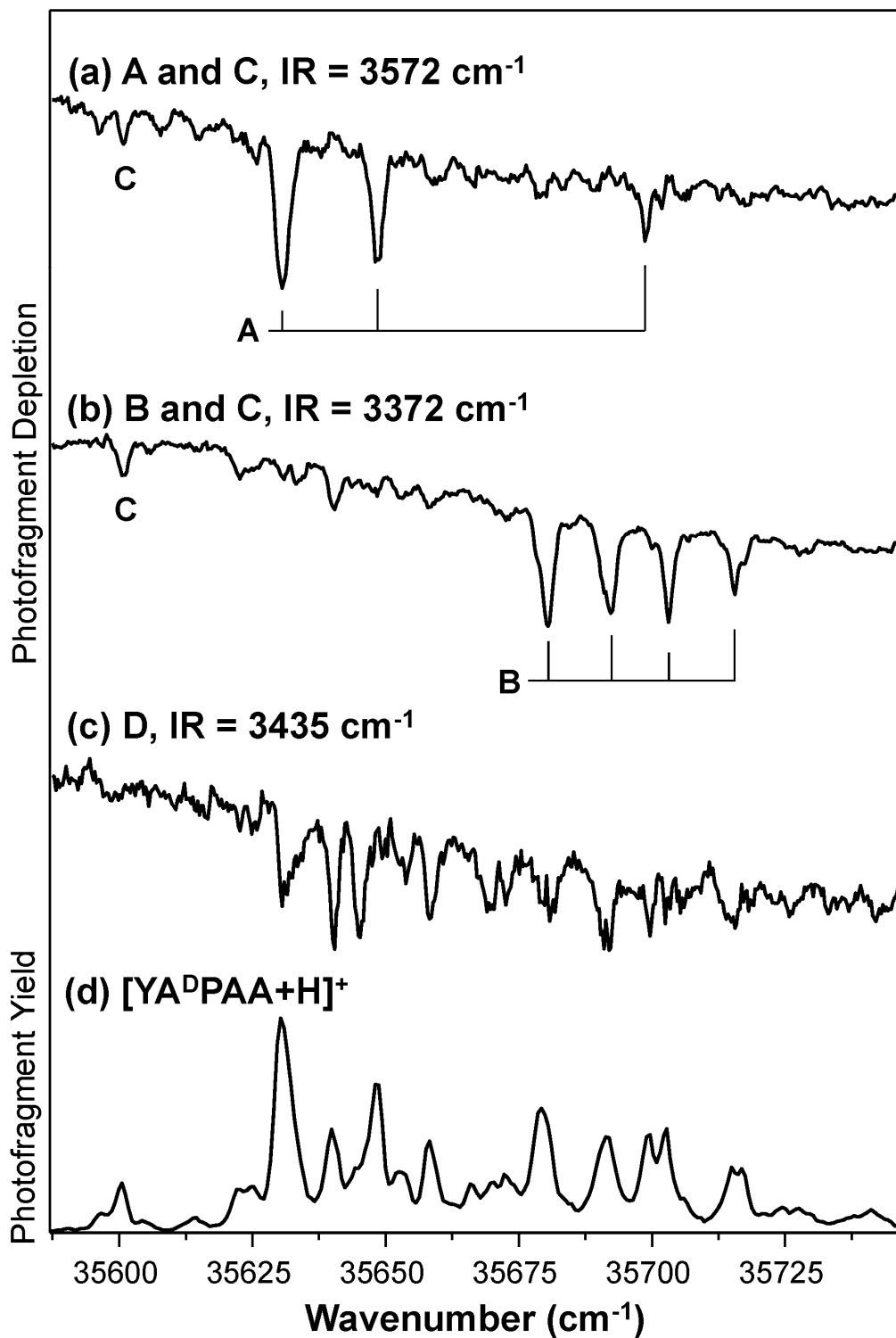
Figure S.8. Conformation-specific UV spectra taken by IR-UV hole-burning. The IR laser was fixed at the acid free OH stretch at 3572 cm^{-1} (a) to probe conformer A and the NH stretch at 3372 cm^{-1} to probe conformer B. Conformer C had transitions in common with both of these wavelengths and is therefore visible in both (a) and (b). To probe conformer (c), the IR laser was fixed at the NH stretching frequency of 3435 cm^{-1}. These conformation-specific spectra can be compared to the UV action spectrum shown in (d) and account for all of the observed bands.

V. [YA^{D}PAA+H]$^+$ Conformers C and D

A comparison between the experimental and calculated harmonic level spectra of conformers A and C in [YA^{D}PAA+H]$^+$ is given in Figure S.9. As illustrated in Figure S.10, the assigned 3D structures of these conformers are quite similar, differing by a torsion of the tyrosine side chain. Due to the overlap between the origin band of conformer D and a vibronic band of conformer A, we have not been able to record an adequate spectrum of conformer D for a detailed structural assignment. However, we know from the IR gain spectrum [Figure S.6 (a)] that the only distinct transition is the NH stretch at 3435 cm^{-1}, which exhibits a shift to lower wavenumber from the free NH stretch at 3450 cm^{-1}. We also know that this conformer does not contain a free acid OH stretch because it was not observed in the IR-UV hole burning spectrum (Figure S.8) when the IR laser was fixed at 3572 cm^{-1}. Thus, its structure is likely similar to either conformer A or B and contains an H-bonded acid OH group.

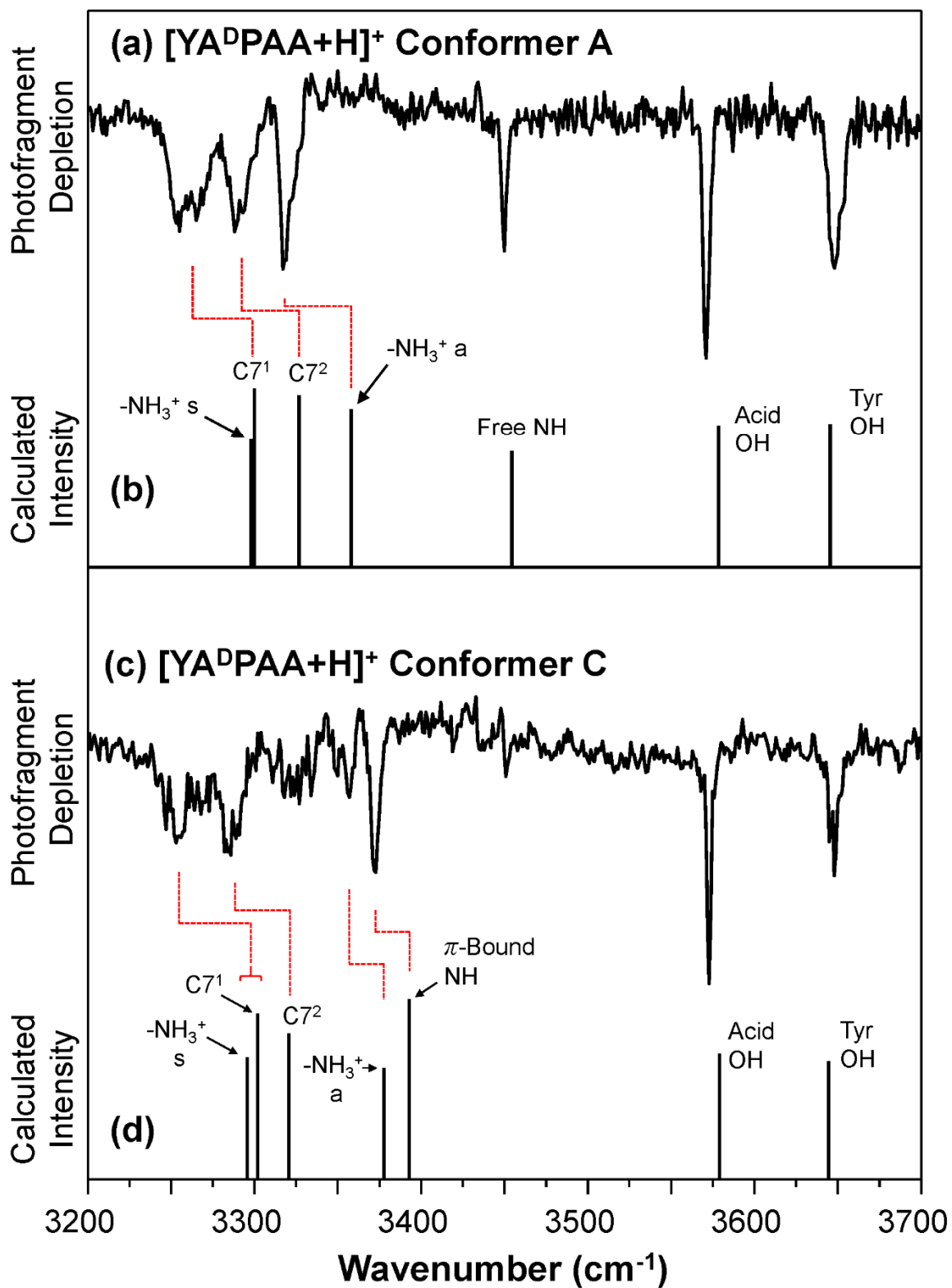**Figure S.9.** A comparison of the conformation-specific IR spectra of conformers A (a) and C (c) of [YA^{D}PAA+H]$^+$. Calculated harmonic level spectra at the B3LYP-GD3BJ/6-31+G* level of theory (NH and CH scaled by 0.958 and free OH scaled by 0.973) are also compared for conformers A (b) and C (d).

(a) [YA^DPAA+H]⁺ Conformer A

(b) [YA^DPAA+H]⁺ Conformer C
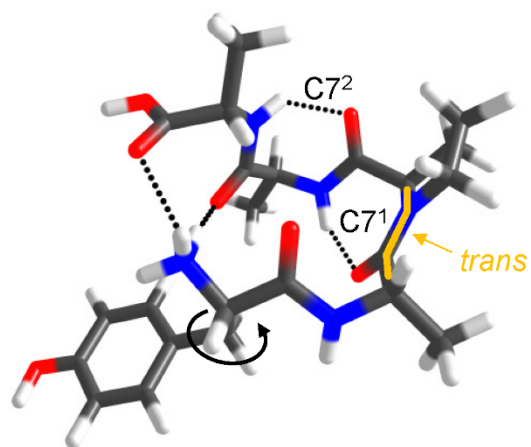
ΔG_{rel} = 0.0 kJ·mol^{-1}
C14,C17,π/F$_{NH}$/*trans*/C7/C7/F$_{OH}$
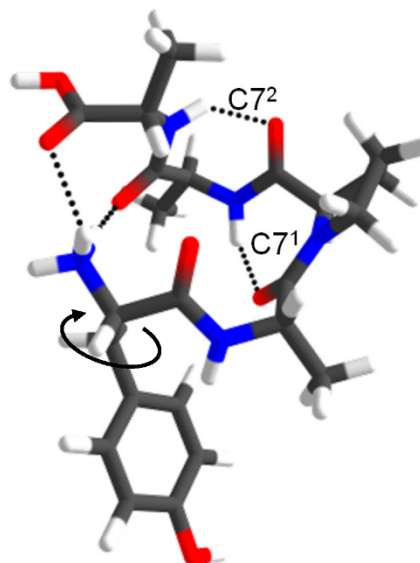
ΔG_{rel} = 2.78 kJ·mol^{-1}
C14,C17,F$_{NH}$/π_{NH}/*trans*/C7/C7/F$_{OH}$

Figure S.10. Assigned structures of conformers A (a) and C (b) of [YA^DPAA+H]$^+$. The relative energies (ΔG_{rel}) are given below each structure as well as the structural nomenclature.

VI. Band Assignments

TABLE S.1: Summary of Experimental ($\pm$ 3 cm^{-1}) and Calculated Band Positions in cm^{-1}

|	Assignment	Exp. Wavenumber	Calc. Wavenumber
[YA^{D}PAA+H]$^+$ Conformer A	Tyr OH	3648	3646
	Acid OH	3571	3579
	Free NH	3450	3454
	NH$_3^+$ a	3317	3358
	C7^2	3288	3327
	C7^1	3260	3300
	-NH$_3^+$ s	3260	3298
	Acid CO	1759, 1767	1760
	Ala$_2$ CO	1644	1653
[YA^{D}PAA+H]$^+$ Conformer B	Tyr OH	3650	3646
	Free NH	3457	3455
	C14	3372	3377
	-NH$_3^+$-π	3292	3323
	C10	3292	3321
	NH$_3^+$ a, s, Acid OH	2850-3100	3105, 3082, 3011
	Acid CO	1729	1740
	Ala$_2$ CO	1641	1647
[YA^{D}PAA+H]$^+$ Conformer C	Tyr OH	3648	3645
	Acid OH	3573	3579
	π-Bound NH	3373	3393
	-NH$_3^+$ a	3357	3378
	C7^2	3284	3320
	C7^1	3253	3302
	-NH$_3^+$ s	3253	3295
[YA^{L}PAA+H]$^+$	Tyr OH	3645	3645
	Acid OH	3571	3578
	Free NH	3446	3464
	C5	3397	3413
	-NH$_3^+$ a	3320	3356
	C7	3320	3348
	-NH$_3^+$ s	3259	3297
	-NH$_3^+$ C14	2600-3150	2924
	Acid CO	1769	1763
	Ala^2 CO	1676	1687
[YG^{L}PAA+H]$^+$ *trans* Acid	Tyr OH	3647	3645
	Free NH	3483	3475
	C10	3417	3427
	C7	3306	3329
	-NH$_3^+$-π	3228	3251
	Acid OH	3030	3120
	-NH$_3^+$ C14	2936	3050
	-NH$_3^+$ C17	2827	3028

	Acid CO	1745	1751
[YG^{L}PAA+H]$^+$ *cis* Acid	Tyr OH	3643	3645
	Free NH	3471	3468
	C10	3389	3404
	C7	3326	3333
	-NH$_3^+$-π	3248	3281
	Acid OH	3010	3157
	-NH$_3^+$ C14	3010	3100
	-NH$_3^+$ C17	2855	2993
	Acid CO	1725	1734

VII. Comparison of Zero-Point (0 K) and Free Energy (298 K) Corrected Structures
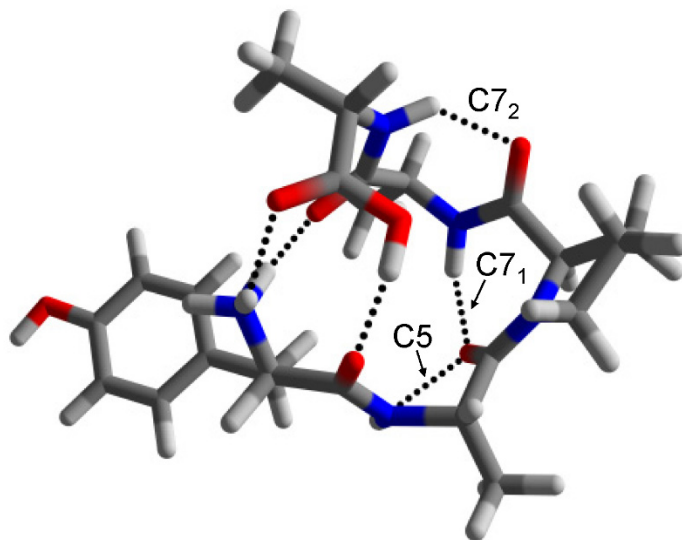
$C14,C17,\pi/C5/trans/C7/C7/C16_{OH}$

Figure S.11. Calculated global minimum structure of $[YA^{D}PAA+H]^+$ at 0 K. At 298 K, $\Delta G_{rel} = 0.26$ kJ·mol^{-1}

TABLE S.2: Relative Energies and Structural Names of [YA^{D}PAA+H]$^+$ and [YA^{L}PAA+H]$^+$ Conformers Calculated at the B3LYP-GD3BJ/6-31+G* Level of Theory

		YA^{D}PAA			YA^{L}PAA	
	ΔG at 298 K (kJ/mol)	ZPE Corrected (kJ·mol^{-1})	Structure Name	ΔG at 298 K (kJ/mol)	ZPE Corrected (kJ·mol^{-1})	Structure Name
A	0.00	4.38	C14,C17,π_{NH}/F$_{NH}$/*trans*/C7/C7/F$_{OH}$	14.82	21.32	C14,C17,π_{NH}/C5/*cis*/C5$_N$/C7/F$_{OH}$
	0.26	0	C14,C17,π_{NH}/C5/*trans*/C7/C7/C16$_{OH}$	15.52	22.20	C14,C17,π_{NH}/C5/*cis*/C5$_N$/C7/F$_{OH}$
	0.39	4.96	C14,C17,π_{NH}/F$_{NH}$/*trans*/C7/C7/F$_{OH}$	19.12	22.09	C14,C17,π_{NH}/C5/*cis*/C5$_N$/C7/C16$_{OH}$
	1.03	0.71	C14,C17,π_{NH}/C5/*trans*/C7/C7/C16$_{OH}$	19.74	22.97	C14,C17,π_{NH}/C5/*cis*/C5$_N$/C7/C16$_{OH}$
	1.64	2.02	C11,C17,π_{NH}/C14/*trans*/F$_{NH}$/C5/C13$_{OH}$	21.50	27.54	C14,C17,F$_{NH}$/π_{NH}/*cis*/C5/C7/F$_{OH}$
	2.37	2.97	C11,C17,π_{NH}/C14/*trans*/F$_{NH}$/C5/C13$_{OH}$	22.55	28.65	C14,C17,F$_{NH}$/π_{NH}/*cis*/C5$_N$/C7/F$_{OH}$
	2.63	1.81	(C14,C5),C17,π_{NH}/F$_{NH}$/*trans*/C10/C7/C13$_{OH}$	22.65	27.72	C5,C17,π_{NH}/C14/*trans*/F$_{NH}$/C7/C7$_{OH}$
	2.68	4.45	C14,C17,F$_{NH}$/π_{NH}/trans/C7/C7/F$_{OH}$	22.81	19.96	C14,C17,F$_{NH}$/π_{NH}/*cis*/C10/C7/C13$_{OH}$
C	2.78	4.76	C14,C17,F$_{NH}$/π_{NH}/*trans*/C7/C7/F$_{OH}$	23.10	27.96	C5,C17,π_{NH}/C14/*trans*/F$_{NH}$/C7/C7$_{OH}$
	2.83	1.9	C14,C17,π_{NH}/F$_{NH}$/*trans*/C10/C7/C13$_{OH}$	25.78	25.64	C11,C14,π_{NH}/C14/*cis*/C5$_N$/C5/C13$_{OH}$
B	3.15	2.96	C11,C17,π_{NH}/C14/*trans*/F$_{NH}$/C10/C7$_{OH}$	26.03	28.56	C14,C17,F$_{NH}$/π_{NH}/*cis*/C5$_N$/C7/C16$_{OH}$
	3.18	3.3	C11,C17,π_{NH}/C14/*trans*/F$_{NH}$/C10/C7$_{OH}$	26.55	29.38	C14,C17,F$_{NH}$/π_{NH}/*cis*/C5$_N$/C7/C16$_{OH}$
	3.69	7.31	C11,C17,π_{NH}/C14/*trans*/F$_{NH}$/C10/F$_{OH}$	26.90	24.4	C14,C17,π_{NH}/F$_{NH}$/*trans*/(C5$_N$,C10)/C7/C13$_{OH}$
	3.91	2.43	C14,C17,F$_{NH}$/π_{NH}/*trans*/C7/C7/C16$_{OH}$	26.92	30.24	C5,C17,F$_{NH}$/π_{NH}/*cis*/C5$_N$/F$_{NH}$/C16$_{OH}$
	3.93	2.32	C14,C17,F$_{NH}$/π_{NH}/*trans*/C7/C7/C16$_{OH}$	27.07	19.47	C11,C14,F$_{NH}$/C11/*cis*/C5$_N$/F$_{NH}$/C13$_{OH}$
	6.00	5.9	C14,C17,F$_{NH}$/π_{NH}/*trans*/C7/F$_{NH}$/C10$_{OH}$	27.07	30.18	C5,C17,π_{NH}/C14/*trans*/C5$_N$/C7/C7$_{OH}$
	6.03	5.58	C11,C17,π_{NH}/C14/*trans*/F$_{NH}$/C10/C7$_{OH}$	27.24	27.06	C11,C14,π_{NH}/C14/*cis*/C5$_N$/C5/C13$_{OH}$
	6.71	3.91	C14,C17,F$_{NH}$/π_{NH}/*trans*/C10/C7/C13$_{OH}$	27.61	30.79	C5,C17,π_{NH}/C14/*trans*/C5$_N$/C7/C7$_{OH}$
	6.94	4.16	C14,C17,F$_{NH}$/π_{NH}/*trans*/C10/C7/C13$_{OH}$	28.67	32.9	C5,C17,π_{NH}/C5/*trans*/F$_{NH}$/C7/C7$_{OH}$
	9.45	7.34	C14,C17,π_{NH}/F$_{NH}$/*trans*/C10/C7/C13$_{OH}$	29.45	26.77	C14,C17,π_{NH}/F$_{NH}$/*trans*/(C5$_N$,C10)/C7/C13$_{OH}$
	9.66	6.42	C14,C17,π_{NH}/F$_{NH}$/*trans*/C10/F$_{NH}$/C13$_{OH}$	29.80	26.56	C14,C17,F$_{NH}$/π_{NH}/*trans*/(C5$_N$,C10)/C7/C13$_{OH}$
	10.11	8.15	C14,C17,π_{NH}/F$_{NH}$/*trans*/C10/C7/C13$_{OH}$	30.27	31.7	(C11,C14),C17,π_{NH}/C14/*cis*/F$_{NH}$/C5/C13$_{OH}$
	10.31	7.24	C14,C17,π_{NH}/F$_{NH}$/*trans*/C10/C7/C13$_{OH}$	30.62	27.54	C14,C17,F$_{NH}$/F$_{NH}$/*trans*/(C5$_N$,C10)/C7/C13$_{OH}$
	12.10	10.51	C5,C17,F$_{NH}$/C8/*trans*/F$_{NH}$/C10/C7$_{OH}$	31.55	34.3	C14,C17,π_{NH}/F$_{NH}$/*cis*/C8/C5/C13$_{OH}$
	13.92	10.1	C14,C17,F$_{NH}$/π_{NH}/*trans*/C10/C7/C13$_{OH}$	31.68	30.14	C14,C17,π_{NH}/F$_{NH}$/*trans*/(C5$_N$,C10)/C7/C13$_{OH}$
	13.93	9.91	C14,C17,F$_{NH}$/π_{NH}/*trans*/C10/C7/C13$_{OH}$	31.91	33.1	C14,C17,F$_{NH}$/π_{NH}/*cis*/(C5$_N$,C8)/F$_{NH}$/C13$_{OH}$
	13.98	15.05	C14,C17,π_{NH}/C5/*trans*/C7/F$_{NH}$/C10$_{OH}$	33.22	33.05	C14,C17,F$_{NH}$/F$_{NH}$/*trans*/(C5$_N$,C10)/C7/C13$_{OH}$
	14.00	10.93	C14,C5/C5/*trans*/C7/C7/C16$_{OH}$	35.70	36.58	C5,C11,π_{NH}/C14/*trans*/F$_{NH}$/C10/C7$_{OH}$
	15.24	16.51	C14,C17,π_{NH}/C5/*trans*/C7/C7/C10$_{OH}$	38.99	40.1	C8,C14,(C17,π_{NH})/F$_{NH}$/*trans*/C5$_N$/C7/C10$_{OH}$

17.04	18.08	C14,C17,F_{NH}/π_{NH}/*trans*/C7/F_{NH}/C10$_{OH}$
17.42	18.47	C14,C17,F_{NH}/π_{NH}/*trans*/C7/F_{NH}/C10$_{OH}$
28.07	28.82	C5,C11,(C17,π_{NH})/C11/*cis*/C5$_N$/F_{NH}/π_{NH}
29.58	30.37	C5,C11,(C17,π_{NH})/C11/*cis*/C5$_N$/F_{NH}/π_{NH}
32.40	33.96	C5,C11,(C17,π_{NH})/C11/*cis*/C5$_N$/F_{NH}/π_{NH}
35.45	40.44	C5,C11,(C17,π_{NH})/C11/*cis*/C5$_N$/F_{NH}/F_{OH}
40.40	45.94	C5,C11,(C17,π_{NH})/C11/*cis*/C5$_N$/F_{NH}/F_{OH}

TABLE S.3: Relative Energies and Structural Names of [YGPAA+H]$^+$ Conformers Calculated at the B3LYP-GD3BJ/6-31+G* Level of Theory

YGPAA		
ΔG at 298 K (kJ/mol)	ZPE Corrected (kJ·mol^{-1})	Structure Name
0.00	1.56	C14,C17,π_{NH}/F_{NH}/*trans*/C10/C7/C13$_{cOH}$//*syn*,P1[a]
0.19	1.56	C14,C17,π_{NH}/F_{NH}/*trans*/C10/C7/C13$_{cOH}$//*anti*,P1
0.66	0.00	C14,C17,π_{NH}/F_{NH}/*trans*/C10/C7/C13$_{tOH}$//*syn*,P2
0.73	0.05	C14,C17,π_{NH}/F_{NH}/*trans*/C10/C7/C13$_{tOH}$//*anti*,P2
0.80	1.07	C14,C17,π_{NH}/F_{NH}/*trans*/C10/C7/C13$_{tOH}$//*syn*,P1
0.93	1.11	C14,C17,π_{NH}/F_{NH}/*trans*/C10/C7/C13$_{tOH}$//*anti*,P1
4.19	3.60	C14,C17,F_{NH}/π_{NH}/*trans*/C10/C7/C13$_{tOH}$//*anti*,P2
4.19	7.02	C14,C17,π_{NH}/F_{NH}/*trans*/C10/C7/C13$_{cOH}$//*syn*,P2
4.36	7.05	C14,C17,π_{NH}/F_{NH}/*trans*/C10/C7/C13$_{cOH}$//*anti*,P2
5.01	7.15	C14,C17,F_{NH}/π_{NH}/*trans*/C10/C7/C13$_{cOH}$
5.35	5.11	C14,C17,π_{NH}/F_{NH}/*trans*/C10/C7/C13$_{tOH}$
5.67	7.86	C14,C17,F_{NH}/π_{NH}/*trans*/C10/C7/C13$_{cOH}$
5.71	5.01	C14,C17,F_{NH}/π_{NH}/*trans*/C10/C7/C13$_{tOH}$
6.18	6.54	C14,C17,π_{NH}/F_{NH}/*trans*/C10/C7/C13$_{tOH}$
6.34	6.40	C14,C17,F_{NH}/π_{NH}/*trans*/C10/C7/C13$_{tOH}$
6.85	7.92	C14,C17,π_{NH}/F_{NH}/*trans*/C10/C7/C13$_{tOH}$
7.23	7.79	C14,C17,F_{NH}/F_{NH}/*trans*/C10/C7/C13$_{tOH}$
8.08	9.23	C14,C17,π_{NH}/F_{NH}/*trans*/C10/C7/C13$_{cOH}$
9.01	8.84	C14,C17,F_{NH}/F_{NH}/*trans*/C10/C7/C13$_{cOH}$
10.08	10.20	C14,C17,F_{NH}/F_{NH}/*trans*/C10/C7/C13$_{cOH}$
16.25	17.70	C5,C14,π_{NH}/C14/*trans*/F_{NH}/C5/C13$_{cOH}$
20.38	19.92	C14,C17,π_{NH}/C5/*cis*/C10/C7/C13$_{cOH}$
20.71	20.23	(C5,C14),C17,π_{NH}/F_{NH}/*cis*/C10/C7/C13$_{cOH}$
23.32	25.48	C11,C17,π_{NH}/C14/*trans*/F_{NH}/C10/C7$_{tOH}$
24.43	32.28	C5,C14,π_{NH}/C5/*cis*/F_{NH}/C7/F_{OH}
25.51	29.61	C14,C17,π_{NH}/C5/*cis*/F_{NH}/C7/C16$_{cOH}$

25.86	28.04	$C11,C14,\pi_{NH}/C14/cis/F_{NH}/C5/C13_{cOH}$
26.18	30.56	$C14,C17,\pi_{NH}/C5/cis/F_{NH}/C7/C16_{cOH}$
27.33	29.50	$C11,C14,\pi_{NH}/C14/cis/F_{NH}/C5/C13_{cOH}$
28.37	33.06	$C17,F_{NH},F_{NH}/\pi_{NH}/cis/F_{NH}/C7/C16_{cOH}$
28.77	33.60	$C14,C17,\pi_{NH}/C5/cis/F_{NH}/C7/C16_{cOH}$
29.33	34.51	$C14,C17,\pi_{NH}/C5/cis/F_{NH}/C7/C16_{cOH}$
29.82	34.43	$C17,F_{NH},F_{NH}/\pi_{NH}/cis/F_{NH}/C7/C16_{cOH}$
31.62	30.61	$C17,C17,F_{NH}/F_{NH}/cis/F_{NH}/C7/C7_{tOH}$
32.83	36.43	$C14,C17,F_{NH}/\pi_{NH}/cis/F_{NH}/C7/C16_{cOH}$
34.57	37.57	$C11,C17,\pi_{NH}/C14/cis/F_{NH}/F_{NH}/C13_{cOH}$
35.27	38.74	$C11,C17,\pi_{NH}/C14/cis/F_{NH}/F_{NH}/C13_{cOH}$
40.61	46.51	$C11,C14,F_{NH}/C10/cis/F_{NH}/C5/F_{OH}$

[a] In the lowest energy structures (<5 kJ·mol⁻¹), differences in the sidechain conformations are represented after the double slashes (//). The labels *anti* and *syn* denote the relative orientation of the Tyr OH group with respect to the $-NH_3^+$ group, while P1 and P2 denote different "puckering" isomers of the proline ring.

VIII. Conformer-Specific IR Spectrum of [YA^{D}PAA+H]$^+$ in the Electronic Excited State

To gain further insight to the structure of conformer A of the [YA^{D}PAA+H]$^+$ species, we took IR spectra in the excited electronic state as a means of probing which transitions are affected by electronic excitation and therefore are associated with groups in close proximity to the Tyr aromatic ring. Infrared spectra in the electronic excited states have been taken of several neutral biomolecules containing aromatic groups.[6] Similarly, Rizzo and coworkers[3] have also recorded vibrational spectra of cryocooled peptide ions containing Tyr and Phe in their electronic excited state simply by delaying the IR excitation to occur immediately following the UV excitation, rather than before it. These spectra can either be taken while the excited state population is in the S_1 or T_n states depending on this delay time (*e.g.*, <20 ns for S_1 and >20 ns for T_1 but highly system dependent). We employed this technique on conformer A of [YA^{D}PAA+H]$^+$ because Rizzo and coworkers[3] observed selective shifts to lower wavenumber of the -NH$_3^+$ stretches that are bound to the π-cloud.

The excited state IR spectrum of conformer A is shown in Figure S.12. In this example, the IR laser was delayed to occur 20 ns after the UV laser, producing a spectrum that likely contains contributions from both S_1 and T_1 states. As anticipated based on the assigned structure, the most significant changes in the spectrum involve the -NH$_3^+$ *s* and -NH$_3^+$ *a* transitions, which both shift down in frequency and broaden in the electronic excited state. In contrast, the isolated C7^2 NH stretch and free NH stretch fundamentals remain at the same wavenumber. The shoulder on the high wavenumber edge of the acid OH stretch was observed to disappear when the delay was decreased to 8 ns and to dominate when the delay was increased to 100 ns. This result implies that the acid OH stretch is shifted to higher frequency by a few wavenumbers in the T_1 state than in the S_1 or S_0 states, which is likely a consequence of the proximity of the acid group to the Tyr ring in

this folded gas-phase structure. We conclude that the shift/broadening of the NH stretches, indicated by the red guide lines in Figure 6, provides further confirmation of the assignments, which were deduced from the calculated harmonic level spectrum shown in Figure 5(b).
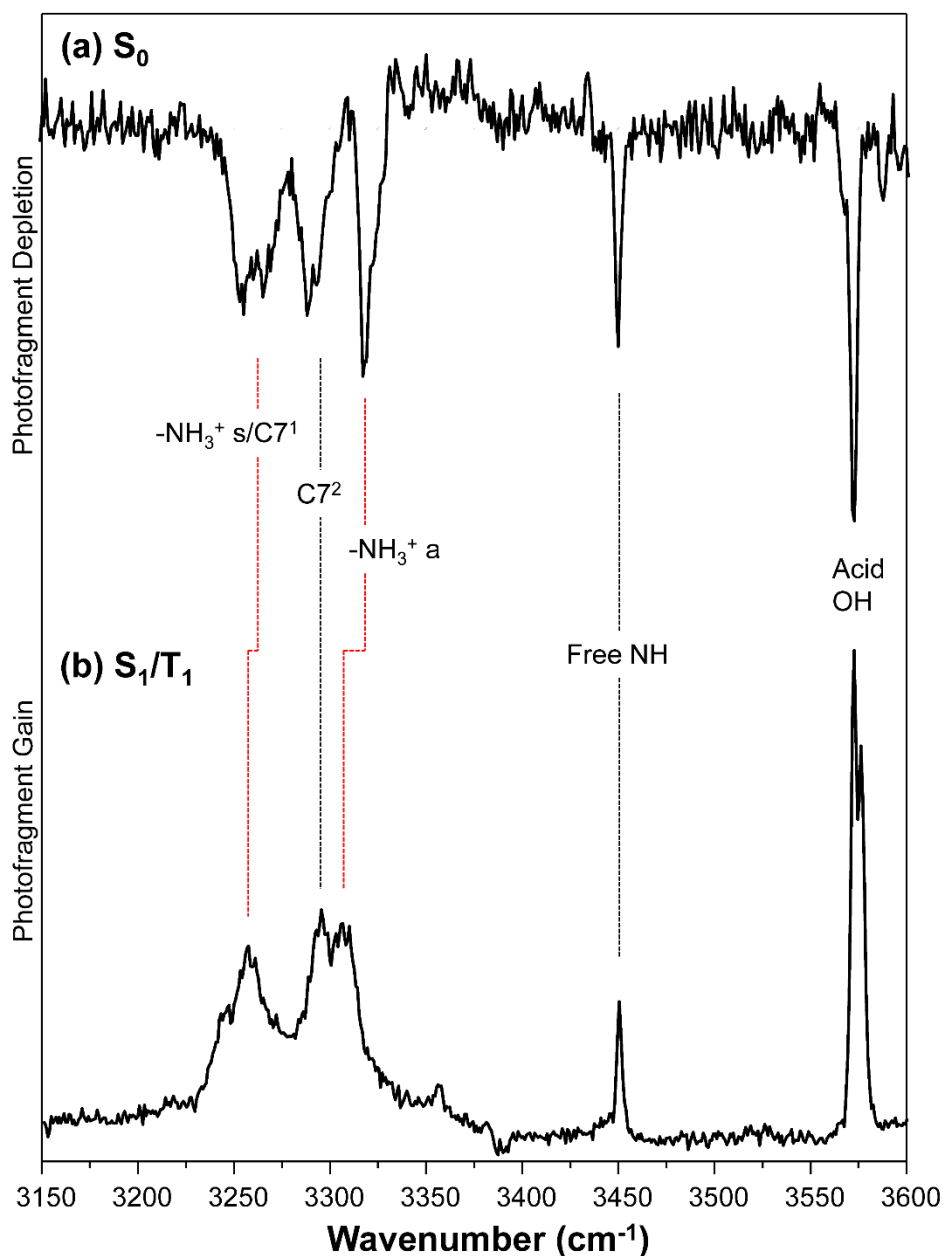

Figure S.12. A comparison of the infrared spectrum of YA^DPAA conformer A in its ground electronic state (a) and electronic excited sate (b). To obtain excited state IR spectra, the IR laser was delayed about 20 ns after the UV laser, resulting in a spectrum that is likely a combination spectra taken in the S_1 and T_1 states.

IX. Zero-Point Corrected Global Minimum of [YA^{L}PAA+H]$^+$

C11,C14,F$_{NH}$/C11/*cis*/C5$_N$/F$_{NH}$/C13$_{OH}$
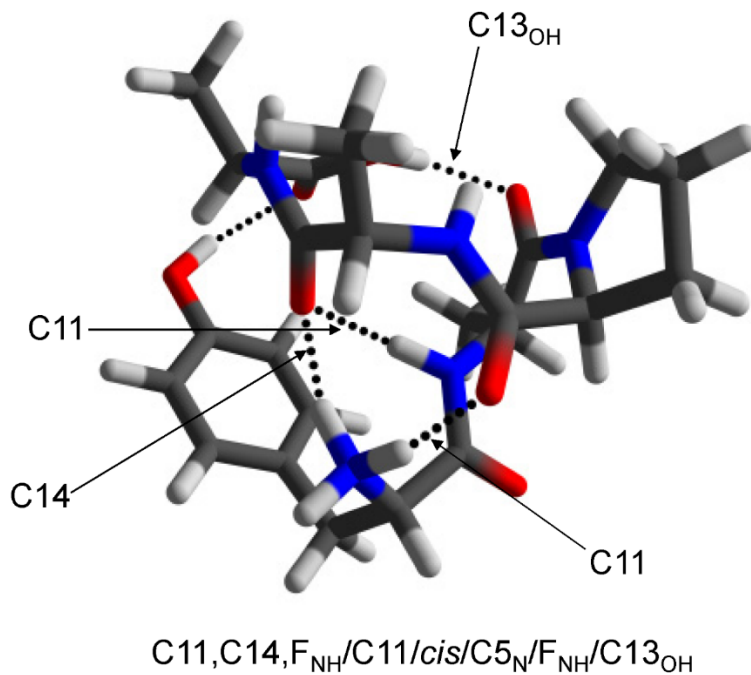
Figure S.13. Calculated zero-point corrected global minimum of [YA^{L}PAA+H]$^+$ at 0 K. At 298 K, ΔG$_{rel}$ is 12.25 kJ·mol^{-1} greater than in the assigned structure.

X. Amide I and II Regions of [YA^{D}PAA+H]$^+$, [YA^{L}PAA+H]$^+$, and [YG^{L}PAA+H]$^+$

Further evidence for the assigned structures of the ^{D}P with ^{L}P diastereomers is gleaned from the carbonyl stretch region of the spectrum. A comparison between the conformation-specific infrared spectra and the calculated vibrational frequencies and IR intensities of the single conformer of [YA^{L}PAA+H]$^+$ and two predominant conformers of [YA^{D}PAA+H]$^+$ is given in Figure S.14. The calculations reproduce the main bands of the spectrum, confirming the assignments based on the hydride stretch spectra.

Upon examination of the structures in Figure 4, it is apparent that the C=O group of the alanine residue adjacent to the tyrosine (A$_2$) is free in the assigned [YA^{L}PAA+H]$^+$ structure but functions as a hydrogen-bond acceptor in both of the [YA^{D}PAA+H]$^+$ conformers (C7 and C10 H-bonds in conformers A and B, respectively). Thus, we expect that this oscillator should absorb at a higher wavenumber in [YA^{L}PAA+H]$^+$ than in [YA^{D}PAA+H]$^+$. This shift is apparent in the calculated spectra, and reproduced by experiment, as indicated by the red dotted lines in Figure S.14. In both [YA^{L}PAA+H]$^+$ and [YA^{D}PAA+H]$^+$, the acid carbonyl is modestly shifted from its free position (1769 cm^{-1} in [YA^{L}PAA+H]$^+$ $vs.$ 1786 cm^{-1} in [GG+H]$^+$).[7] At present, the origin of the doublet acid carbonyl in [YA^{D}PAA+H]$^+$ in conformer A of [YA^{D}PAA+H]$^+$ is unknown and may arise from Fermi resonance. Alternatively, another conformer in the same structural family could contribute to the spectrum if it absorbs at the same UV wavelength, but possesses a slightly different IR spectrum.
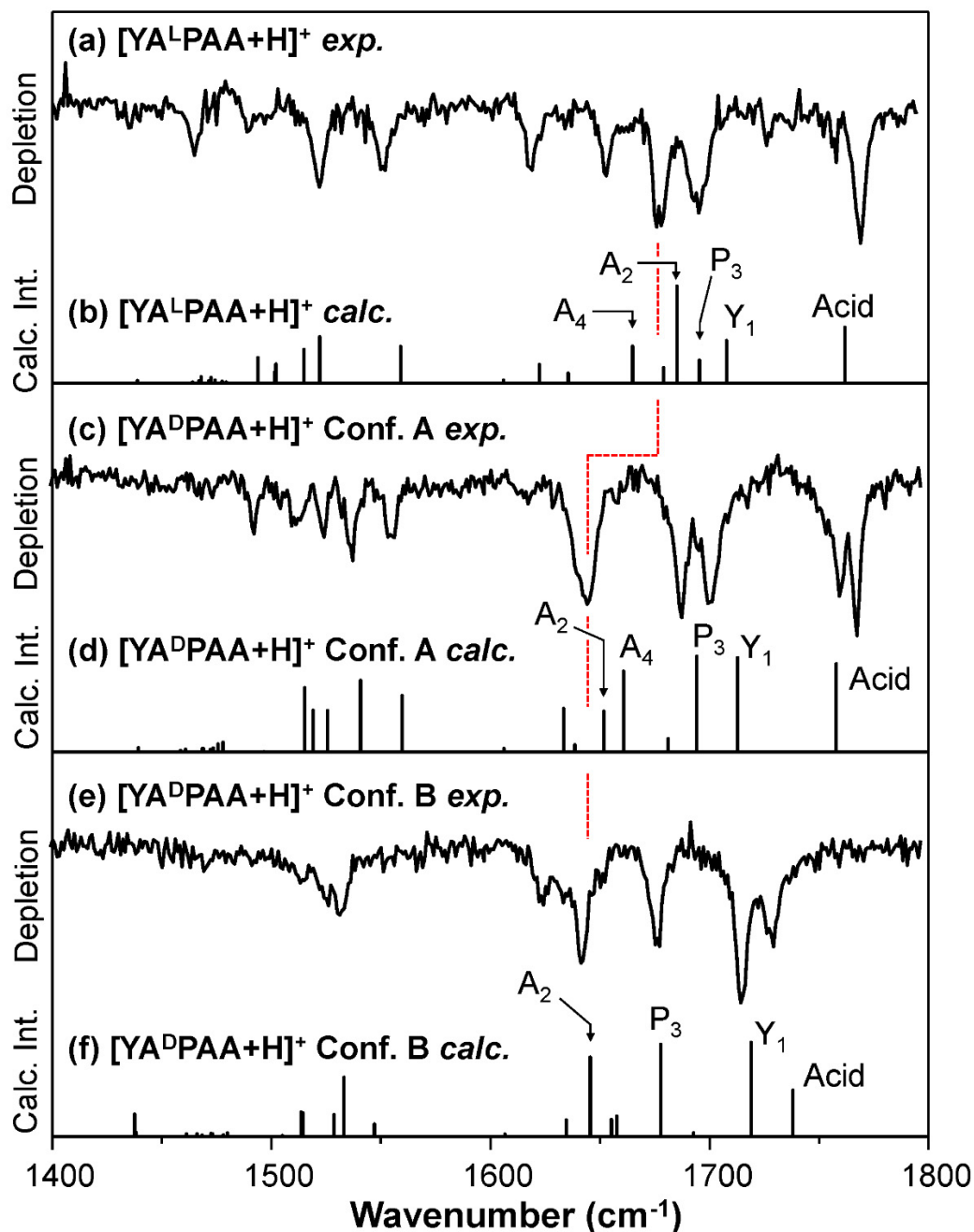
Figure S.14. A comparison of the conformation-specific IR spectra taken by IR-UV double resonance and the calculated harmonic level spectra in the amide I and II regions: [YA^{L}PAA+H]$^+$ experimental (a), [YA^{L}PAA+H]$^+$ calculated (b), [YA^{D}PAA+H]$^+$ conformer A experimental (c), [YA^{D}PAA+H]$^+$ conformer A calculated (d), [YA^{D}PAA+H]$^+$ conformer B experimental (e), [YA^{D}PAA+H]$^+$ conformer B calculated (f). The shift of the CO stretch of the second alanine group (A$_2$) is labeled by the dotted red line and the most intense carbonyl stretches are also labeled according to their corresponding residues (A$_2$, A$_4$, P$_3$, and Y$_1$) in each of the calculated spectra.

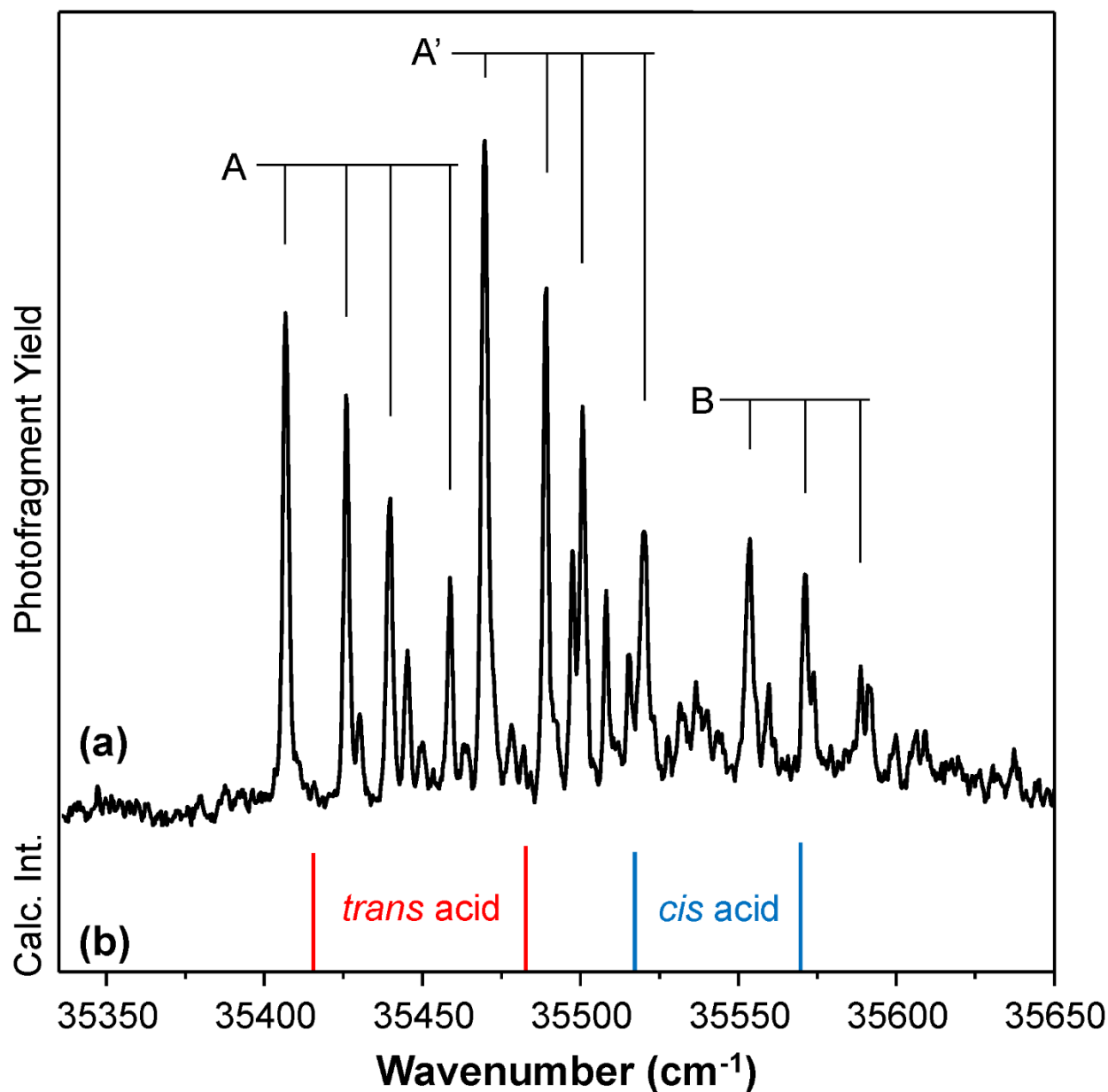# XI. [YG^{L}PAA+H]$^+$ Electronic Spectrum and IR Spectrum in Amide I and II Regions

Figure S.15. A comparison of the UV action spectrum of [YG^{L}PAA+H]$^+$ (a) to the TD-DFT calculated vertical S$_1$←S$_0$ transitions in the assigned *trans* (red) and *cis* (blue) acid structures. These conformers were calculated for two rotamers of the Tyr OH group about the aromatic ring (splittings between the two red sticks and two blue sticks). Also, they are computed to have the same infrared spectrum because the Tyr OH is remote and not involved in H-bonding. Therefore, conformers A and A', which could not be distinguished by IR-UV double resonance spectroscopy, likely correspond to the different Tyr OH rotamers of the *trans* acid structure. The B progression is assigned to the *cis* acid configuration, while the unlabeled bands beneath the A' in the experimental spectrum likely contain contributions from the additional Tyr OH rotamer of this *cis* acid structure.
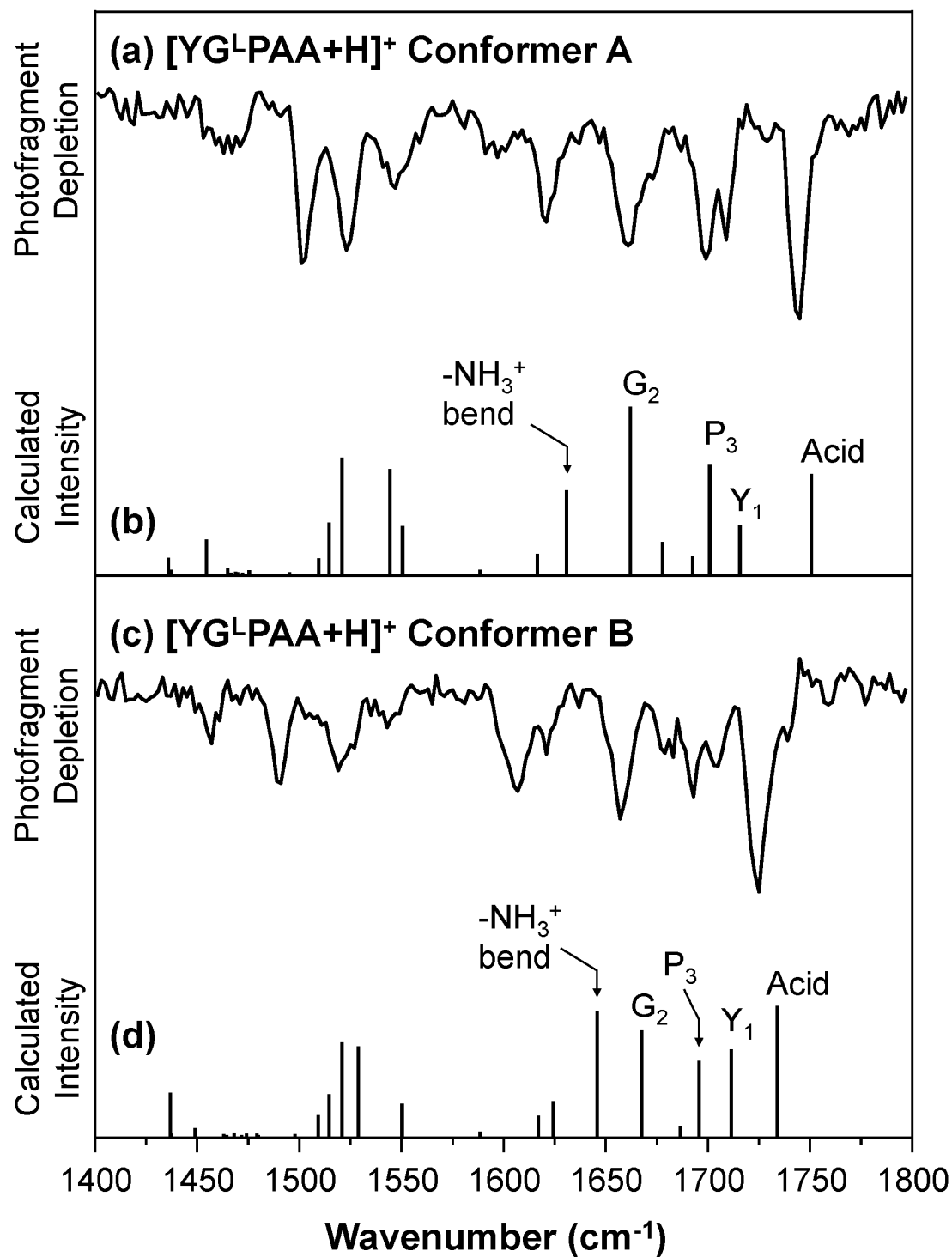
Figure S.16. A comparison of the conformation-specific IR spectra taken by IR-UV double resonance and the calculated harmonic level spectra in the amide I and II regions: [YG^{L}PAA+H]$^+$ experimental (a), [YG^{L}PAA+H]$^+$ calculated (b), [YG^{L}PAA+H]$^+$ conformer B experimental (c), and [YG^{L}PAA+H]$^+$ conformer B calculated (d). The most intense carbonyl stretches are labeled according to their corresponding residues (G$_2$, P$_3$, and Y$_1$) in each of the calculated spectra.

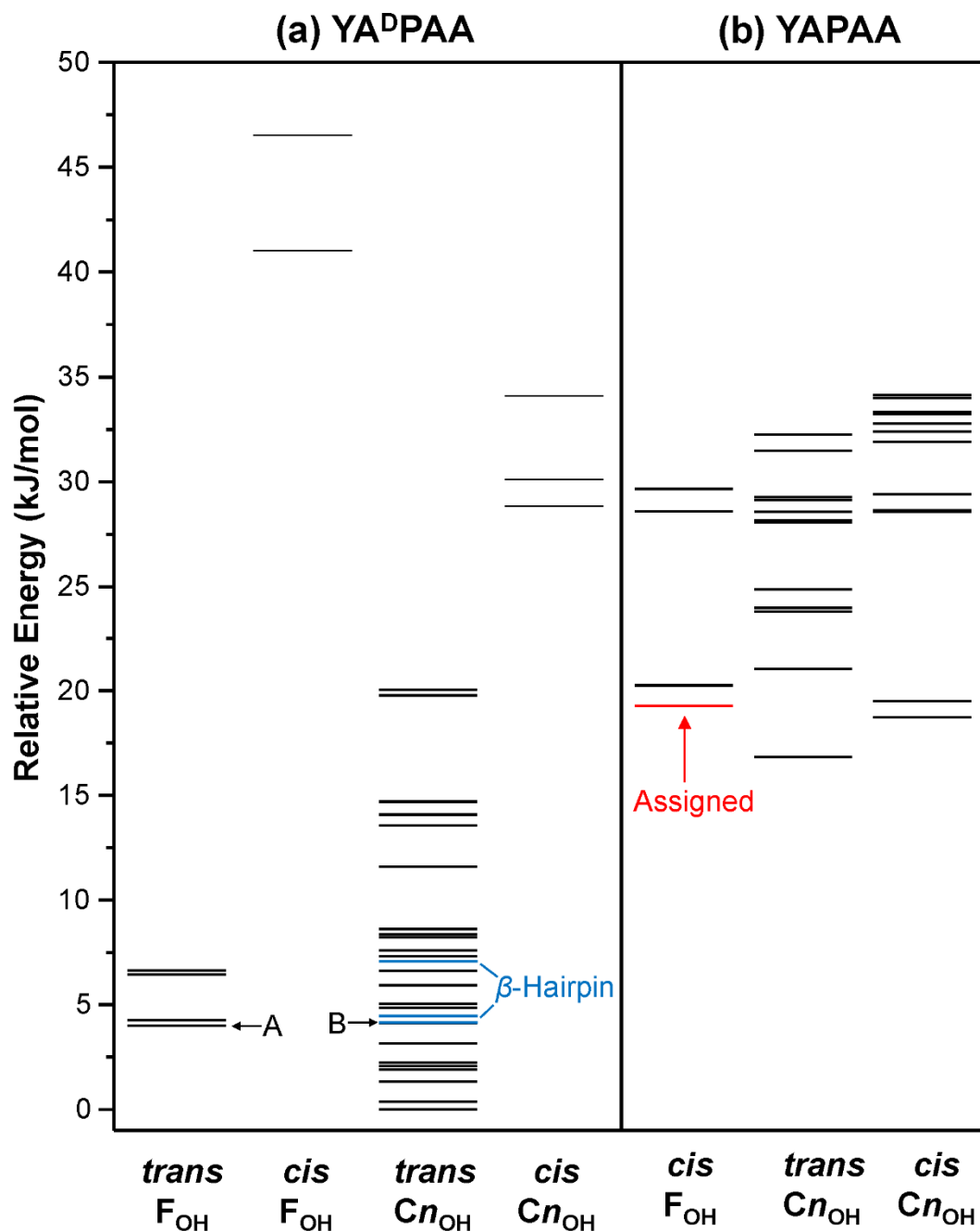**XII. Energy Level Diagrams of [YA$^{D/L}$PAA+H]$^+$**

Figure S.17. Energy level diagrams for [YA^{D}PAA+H]$^+$ (a) and [YA^{L}PAA+H]$^+$ (b), which plot the calculated relative zero-point corrected energies for the various families of conformers at the M05-2X/6-31+G* level of theory. These include *trans* and *cis* configurations of the AP amide bond as well as free (F$_{OH}$) *vs.* cyclic H-bonded (Cn_{OH}) acid OH groups. The blue lines indicate structures in the *β*-hairpin turn family, similar to the one assigned in [YGGFL+H]$^+$. The red line in [YA^{L}PAA+H]$^+$ indicates the global minimum, which is also the assigned structure.
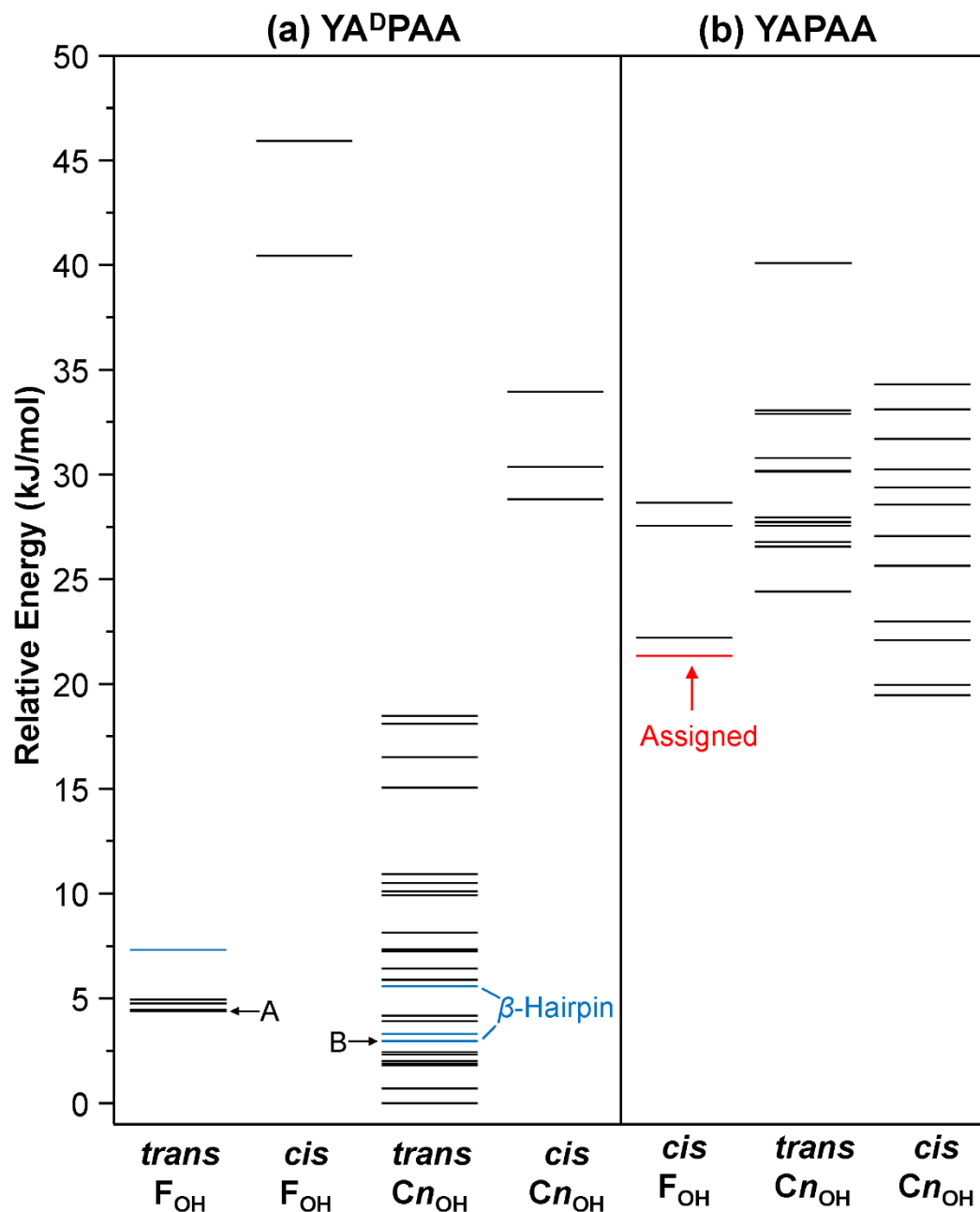
Figure S.18. Energy level diagrams for [YA^{D}PAA+H]$^+$ (a) and [YA^{L}PAA+H]$^+$ (b), which plot the calculated relative zero-point corrected energies for the various families of conformers at the B3LYP-GD3BJ/6-31+G* level of theory. These include *trans* and *cis* configurations of the AP amide bond as well as free (F$_{OH}$) *vs.* cyclic H-bonded (Cn_{OH}) acid OH groups. The blue lines indicate structures in the β-hairpin turn family, similar to the one assigned in [YGGFL+H]$^+$. The red line in [YA^{L}PAA+H]$^+$ indicates the global minimum, which is also the assigned structure.

XIII. Evaluation of the 0 K Global Minimum Structure in [YA^{D}PAA+H]$^+$
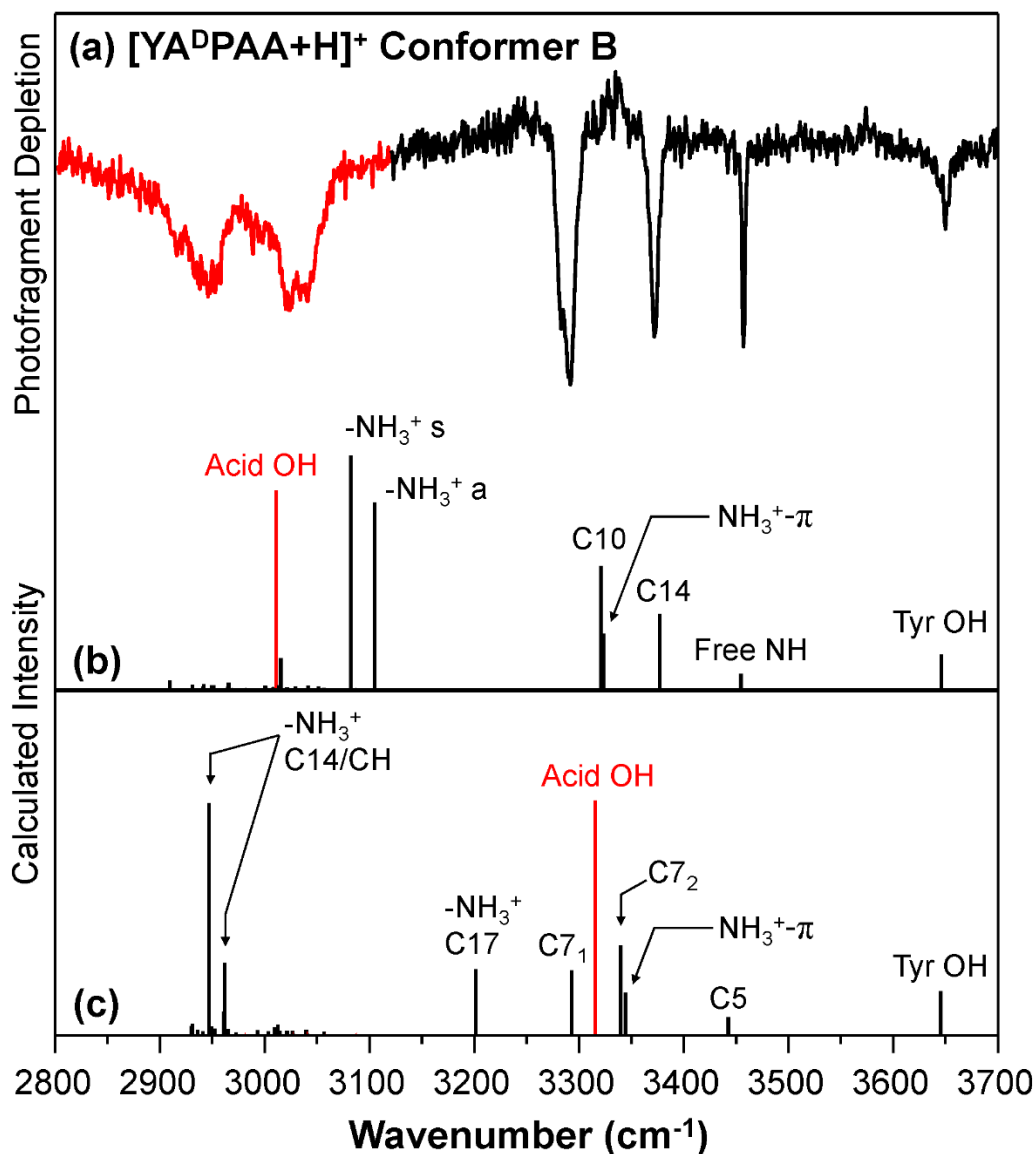

Figure S.19. A comparison of the conformation-specific infrared spectrum of conformer B (a) to the calculated harmonic-level spectra of the assigned Type II' β-turn structure (b) and the global minimum based on zero-point corrected internal energies at 0 K (c). The NH and OH stretches are labeled based on their H-bonding designations as illustrated in Figure 4 for the assigned conformer and Figure S.11 for the 0 K global minimum conformer. For the assigned structure, the acid OH stretch [red stick in (b)] falls within the frequency range of the broad bands in the experimental spectrum, while the acid OH stretch is calculated to exhibit a significant shift to higher wavenumbers in the global minimum conformer (c).

XIV. Energy Level Diagrams of [YGPAA+H]$^+$

Table S.4. Ramachandran Angles of assigned [YAPAA+H]$^+$ and [YGPAA+H]$^+$ Structures

Sequence	ψ_1	ϕ_2	ψ_2	ϕ_3	ψ_3	ϕ_4	ψ_4	ϕ_5	ψ_5
YA^{D}PAA (A)	-169.1	-69.9	139.0	79.3	-78.2	-75.7	79.3	-57.3	-50.8
YA^{D}PAA (B)	-52.4	-88.3	95.6	46.8	-136.0	-67.5	-18.4	-72.3	74.4
YA^{L}PAA	149.5	146.5	143.7	-69.4	-11.2	-77.5	82.8	-54.1	-51.9
YG^{L}PAA (A)	138.7	62.2	-146.0	-54.0	-35.0	-80.1	64.5	46.6	52.9
YG^{L}PAA (B)	141.8	59.1	-134.7	-85.6	-10.5	-85.2	76.8	61.8	67.9

Figure S.20 shows the energy level diagram of [YG^{L}PAA+H]$^+$, plotted as a relative free energy at 298 K. The energy level diagram at 0 K based on zero-point corrected internal energies is given in Figure S.21. It is noteworthy that, once again, the assigned structures are lowest in free energy and well-separated from the higher energy structures that contain different intramolecular H-bonding patterns (structural nomenclature and energies given in Section VII, Table S.3). The other low energy structures that are close in energy to the assigned structures are *cis-trans* conformers of the tyrosine OH group and/or involve puckering of a remote methylene group of the proline ring. Indeed, different proline puckering isomers have been observed in collagen by x-ray crystallography.[8] As the tyrosine OH oscillator is distant and is not involved in H-bonding, the calculated IR spectra of such similar structures are nearly identical. Furthermore, puckering of the proline ring does not change the H-bonding pattern, resulting in very similar calculated spectra. Based on TD-DFT calculations of their differences in vertical excitation energies, the *syn* and *anti* conformers of the Tyr OH group provide a reasonable explanation for several irregular Franck-Condon profiles in the electronic spectra of both [YAPAA+H]$^+$ (Figure S.22) and [YGPAA+H]$^+$ (Figure S.15).

Similar to [YA^DPAA+H]⁺, the energy gap between the *trans-* and *cis-*amide structures is large in [YG^LPAA+H]⁺, with the global minimum *trans* structure 20 kJ·mol⁻¹ lower in energy than the lowest energy *cis* structure. As *cis-*amide structures are lower in energy in the case of [YA^LPAA+H]⁺, we see that both removal of the A_2 methyl group and inversion of the ^LP stereochemistry to ^DP greatly stabilizes structures with *trans* amide bonds. As these *trans-*amide structures differ between [YA^DPAA+H]⁺ and [YG^LPAA+H]⁺, it appears that the pentapeptides is hyper-sensitive to the position of the proline and its surroundings.

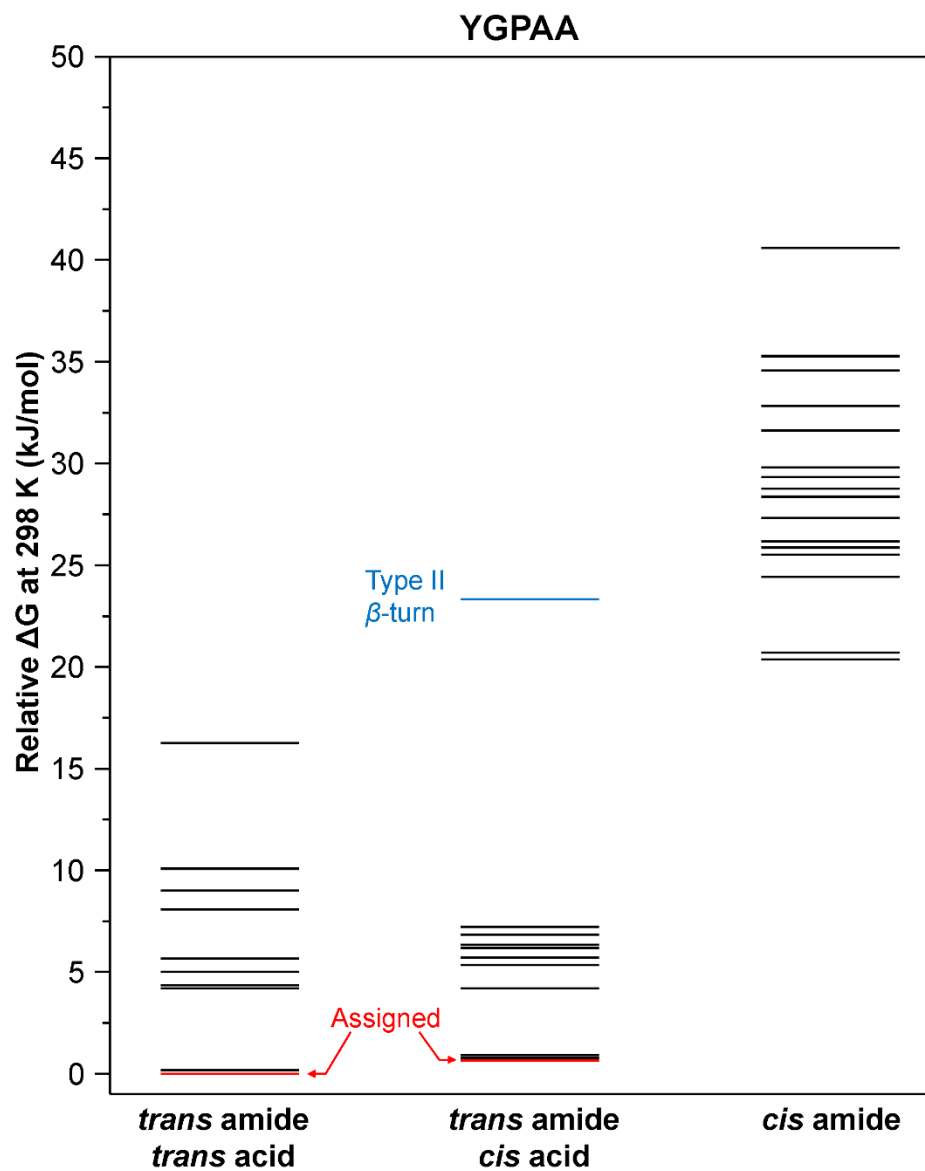**Figure S.20.** Energy level diagram for $[YG^LPAA+H]^+$, which plots the calculated relative ΔG at 298 K for the various families of conformers at the B3LYP-GD3BJ/6-31+G* level of theory. These include *trans* and *cis* configurations of the G^LP amide bond as well as free the acid OH groups. The blue line marks a Type II β-turn structure with the ^LP at the $i+2$ position of the turn and the red lines label the assigned structures.
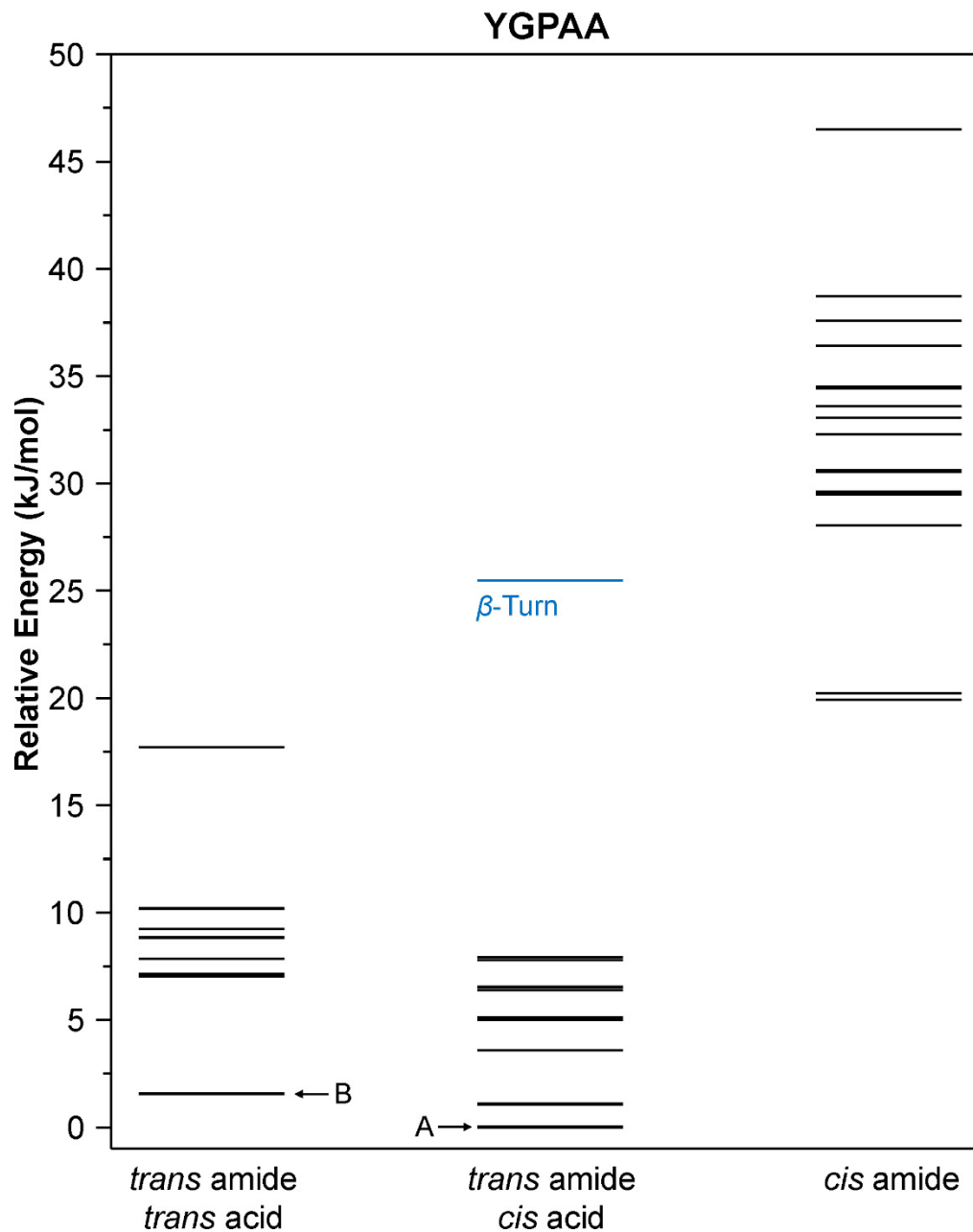
Figure S.21. Energy level diagram for [YG^LPAA+H]^+, which plots the calculated relative zero-point corrected energies for the various families of conformers at the B3LYP-GD3BJ/6-31+G* level of theory. These include *trans* and *cis* configurations of the G^LP amide bond as well as free the acid OH groups. The blue line marks a Type II *β*-turn structure with the ^LP at the *i*+2 position of the turn and the red lines label the assigned structures.

XV. TDDFT Calculations of $[YAPAA+H]^+$

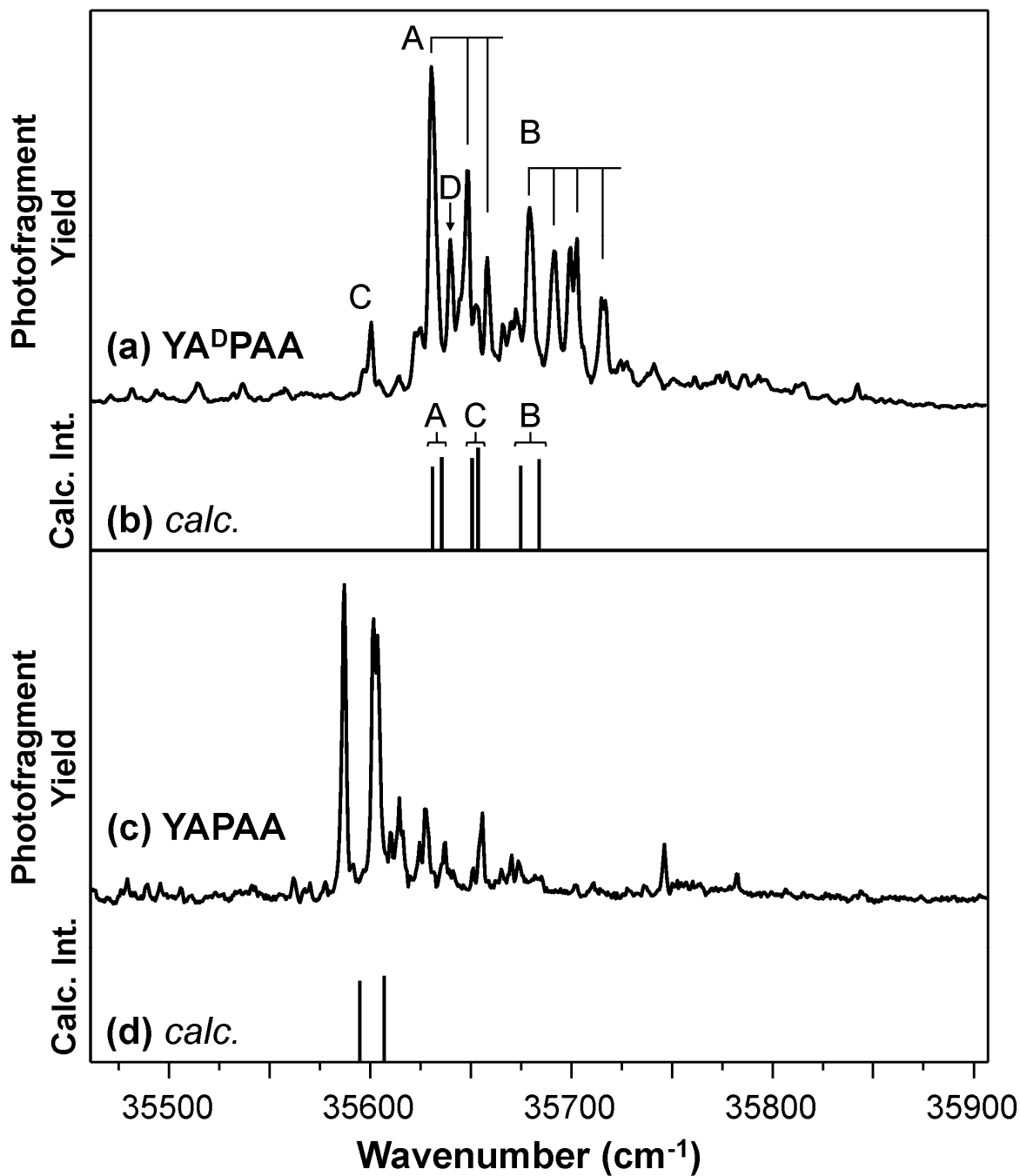**Figure S.22.** A comparison between the calculated TD-DFT $S_1 \leftarrow S_0$ transitions and the experimental spectra of $[YAPAA+H]^+$: UV action spectrum of $[YA^DPAA+H]^+$ (a), calculated $[YA^DPAA+H]^+$ transitions (b), $[YA^LPAA+H]^+$ UV action spectrum (c), and calculated $[YA^LPAA+H]^+$ transitions. The transitions grouped by brackets in (b) and the two calculated transitions in (d) correspond to conformers differing by *cis-trans* isomerization of the Tyr OH group. Such splittings may explain additional non-Franck Condon complexity in the electronic spectra because such pairs of conformers would have indistinguishable infrared spectra. The calculated spectra are scaled by 0.842 for agreement between the calculated and experimentally determined transitions in $[YA^DPAA+H]^+$ conformer A.

References:

(1) Londry, F. A.; Hager, J. W. *J. Am. Soc. Mass Spectrom.* **2003**, *14*, 1130.

(2) Raulfs, M. D. M.; Breci, L.; Bernier, M.; Hamdy, O. M.; Janiga, A.; Wysocki, V.; Poutsma, J. C. *J. Am. Soc. Mass Spectrom.* **2014**, *25*, 1705.

(3) Zabuga, A. V.; Kamrath, M. Z.; Boyarkin, O. V.; Rizzo, T. R. *J. Chem. Phys.* **2014**, *141*, 154309.

(4) Masson, A.; Kamrath, M. Z.; Perez, M. A. S.; Glover, M. S.; Rothlisberger, U.; Clemmer, D. E.; Rizzo, T. R. *J. Am. Soc. Mass Spectrom.* **2015**, *26*, 1444.

(5) Burke, N. L.; Redwine, J. G.; Dean, J. C.; McLuckey, S. A.; Zwier, T. S. *Int. J. Mass Spectrom.* **2015**, *378*, 196.

(6) Buchanan, E. G.; Zwier, T. S. *J. Phys. Chem. A* **2014**, *118*, 8583.

(7) Leavitt, C. M.; DeBlase, A. F.; Johnson, C. J.; van Stipdonk, M.; McCoy, A. B.; Johnson, M. A. *J. Phys. Chem. Lett.* **2013**, *4*, 3450.

(8) Vitagliano, L.; Berisio, R.; Mastrangelo, A.; Mazzarella, L.; Zagari, A. *Protein Sci.* **2001**, *10*, 2627.